LEVEL

AFWAL-TR-81-2055

Michael G. Dunn

MEASUREMENT OF HEAT FLUX AND PRESSURE IN A TURBINE STAGE

CALSPAN ADVANCED TECHNOLOGY CENTER
BUFFALO, NEW YORK 14225

JULY 1981

FINAL REPORT FOR PERIOD JULY 1979 - OCTOBER 1980

Approved for public release; distribution unlimited

AERO-PROPULSION LABORATORY
AIR FORCE WRIGHT AERONAUTICAL LABORATORIES
AIR FORCE SYSTEMS COMMAND
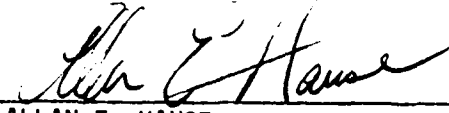WRIGHT-PATTERSON AIR FORCE BASE, OHIO 45433

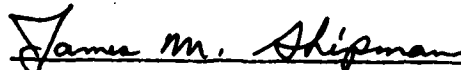This technical report has been reviewed and is approved for publication.

ALLAN E. HAUSE
Project Engineer

JAMES M. SHIPMAN, Major, USAF
Chief, Components Branch

.FOR THE COMMANDER

H. I. BUSH
Acting Director
Turbine Engine Division
Aero Propulsion Laboratory

(9) Final Rept. Jul 79 – Oct 80. /

REPORT DOCUMENTATION PAGE		READ INSTRUCTIONS BEFORE COMPLETING FORM
1. REPORT NUMBER AFWAL-TR-81-2055	2. GOVT ACCESSION NO.	3. RECIPIENT'S CATALOG NUMBER
4. TITLE (and Subtitle) MEASUREMENT OF HEAT FLUX AND PRESSURE IN A TURBINE STAGE.		5. TYPE OF REPORT & PERIOD COVERED July 1979 – October 1980 Technical Report (Final)
		6. PERFORMING ORG. REPORT NUMBER Calspan Report No. 6549-A-2
7. AUTHOR(s) Michael G. Dunn		8. CONTRACT OR GRANT NUMBER(s) F33615-79-C-2075
9. PERFORMING ORGANIZATION NAME AND ADDRESS Calspan Advanced Technology Center 4455 Genesee Street Buffalo, New York 14225		10. PROGRAM ELEMENT, PROJECT, TASK AREA & WORK UNIT NUMBERS 62203F 30660637
11. CONTROLLING OFFICE NAME AND ADDRESS Aero-Propulsion Laboratory (AFWAL/POTC) Air Force Wright Aeronautical Laboratories Wright-Patterson AFB, Ohio 45433		12. REPORT DATE July 1981
		13. NUMBER OF PAGES
14. MONITORING AGENCY NAME & ADDRESS(If different from Controlling Office)		15. SECURITY CLASS. (of this report) UNCLASSIFIED
		15a. DECLASSIFICATION/DOWNGRADING SCHEDULE

16. DISTRIBUTION STATEMENT (of this Report)

Approved for public release; distribution unlimited

17. DISTRIBUTION STATEMENT (of the abstract entered in Block 20, if different from Report)

18. SUPPLEMENTARY NOTES

19. KEY WORDS (Continue on reverse side if necessary and identify by block number)

Full-stage Turbine Heat Transfer
Thin-Film Heat-Transfer Gages
Shroud Static-Pressure Histories

20. ABSTRACT (Continue on reverse side if necessary and identify by block number)
Selected portions of the first-stage stationary inlet nozzle, shroud, and rotor of the AiResearch TFE 731-2 turbine were instrumented with thin-film heat-transfer gages and heat-flux measurements were performed using a shock tunnel as a source of high-temperature, high-pressure gas. Experiments were performed over a range of Reynolds numbers, based on mid-annular stator chord, from 1.6×10^5 to 3.1×10^5 and corrected speeds from approximately 70% to 106%. The full-stage heat-flux results are cast in the form of a Stanton number and are then compared to previous measurements obtained with a stator only,

20. in the absence of a rotor. The previous results are shown to be in good agreement with the full-stage data for the tip end-wall region, but the stator-only Stanton numbers for the stator airfoil are shown to be approximately 20% less than the corresponding full-stage results. Pressure measurements were obtained throughout the model and these results are shown to be in excellent agreement with the steady-state rig data for this turbine. Stanton-number results are also presented for the stationary shroud as a function of rotor mid-annular chord. The shroud Stanton-number data are shown to be in excess of the rotor blade results. Rotor-tip Stanton-number data are likewise shown to be slightly greater than the shroud results.

PREFACE

This report describes an experimental research program conducted by the Calspan Corporation in order to investigate heat-flux distributions on a high-pressure turbine stage.

Accession For

NTIS CRA&I

DTIC T B

Unannounced

Justification

By

Distribution/

Availability Codes

Avail and/or

Dist   Special

A

TABLE OF CONTENTS

LIST OF ILLUSTRATIONS

LIST OF TABLES

viii

NOMENCLATURE

A	stator inlet area
c_s	stator mid-annular chord length
c_r	rotor mid-annular chord length
H_o	total enthalpy
H_w	wall enthalpy
M	Mach number
$\dot{m}$	physical mass-flow rate
N_{phy}	physical rotor speed
N_{corr}	corrected rotor speed, $N_{corr} = N_{phy}/\sqrt{T_o/513}$
$\%N_{corr}$	$N_{corr} \left[(N_{corr})\right]$ design
$\dot{q}$	heat flux
P_o	shock-tube reflected-shock pressure
P_T	total pressure
$R_e)_{c_r}$	Reynolds number based on rotor midchord, $\dfrac{\rho V c_r}{\mu}$
$R_e)_{c_s}$	Reynolds number based on stator midchord, $\dfrac{\rho V c_s}{\mu}$
T_o	total temperature
μ	dynamic viscosity evaluated at T_o
τ_1	defined on Fig. 12
τ_2	defined on Fig. 12
ρV	obtained from $(\dot{m}/A)$

SECTION I
INTRODUCTION

The ability to predict accurately the heat-flux distributions for
various engine components is an important consideration in gas turbine engine
design. Three recent workshops, [1-3] devoted to detailed discussions of the
state of the art of turbine heat-transfer predictive and/or experimental capa-
bility, indicate the necessity for improvement in these areas. In addition to
the work described in [1-3], several calculational techniques, e.g., Dodge [4],
Katsanis [5], Wu [6], Smith [7], Horlock and Perkins [8] and Booth [9], have
been developed. Dodge [10] has compared the results of his 3-D code to the
heat-flux distributions for the early stator-only data [11]. Good agreement
was demonstrated between his predictions and the experimental results.

Many different facilities are currently being used to perform turbine
related studies. These include the long run-time cascade facilities, such as
those used by Blair [12[, Graziani, et al. [13] and York [14], and the low speed
rotating rig of Dring [15]. Also included in the long run-time facility class
would be the new high pressure and temperature combustor and full stage turbine
test facility currently under development at NASA-Lewis as discussed by Stepka
[1]. Many other groups have used, and are still using, short-duration facilities
similar to that used in the present study. Louis [16, 17] has used thin-film
heat-transfer gages to obtain heat-flux measurements on turbine components with
a blow-down facility as the source of test gas. Jones, Schultz, et al. at
Oxford University [18-21] have also used the thin-film heat-transfer gage
techniques but with a light-piston technique as the supply of test gas. This
particular group has performed detailed aerodynamic measurements within their
test environment in order to establish the validity of the short-duration
technique.

All of the facilities and measurement techniques noted above have
applicability to turbine technology development, as there is not a single facility
that meets all of the needs of the turbine designer. The test apparatus used for
the present experiments provides an experimental capability fitting between the
well-known cascade-type facility and the full-scale engine facility.

1

This report describes heat-flux and pressure measurements that were obtained using state of the art shock-tube technology and well established transient-test techniques (thin-film gages and fast-response pressure transducers). These measurements were performed for a full turbine stage of the AiResearch TFE 731-2 engine. This work is an extension of earlier measurements reported in [11] and [22]. These earlier results, obtained for a single stator stage in the absence of a rotor, will be used extensively herein for comparison purposes.

The shock-tunnel facility used provides a clean, uniform, and well-known gas-dynamic condition at the inlet to the stationary nozzle. The experimental technique is not intended to duplicate every known parameter important to turbine heat-transfer studies, but the flow conditions are sufficiently well defined and enough parameters are duplicated so that the measured heat-flux distributions can be used to validate and improve confidence in the accuracy of full-stage design data and existing/advanced predictive techniques under development. In addition, these experimental results have been utilized in the placement of instrumentation for other on-going measurement programs.

SECTION II

EXPERIMENTAL APPARATUS

The experimental apparatus sketched in Figure 1 consists of an 0.20 meter (8-inch) i.d. helium-driven shock tube, consisting of a 12.19-meter (40-foot) long driver tube and a 15.24-meter (50-foot) long driven tube, as a short-duration source of high-temperature, high-pressure air, driving a test-section device mounted near the exit of the primary shock-tunnel nozzle. The receiver tank is initially evacuated to a pressure of approximately 5 torr in order to minimize the starting air load on the turbine wheel and to improve the flow establishment characteristics of the model. It was not possible to reduce further the initial pressure in the receiver because of air leakage from the slip-ring shaft seal. The combination of a large diameter driven tube and very long driver tube accounts for the long test times ($\sim$12 ms) obtained for this work. The test-section device sketched in Figure 2 consists of a forward transition section with a circular opening facing the supersonic primary nozzle flow. The circular opening is followed by a complete 360°-annular passage containing the nozzle stator, the rotor, and the shroud as can be seen in Fig. 2. The rotor-blade tip-to-shroud clearance at 0 rpm was constructed to be 5.1×10^{-4}-meters (0.020-inches). Because the rotor will increase in diameter by about 2.0×10^{-4}-meters (0.008-inches) during operation, the actual clearance when the wheel is at full speed is on the order of 3.0×10^{-4}-meters (0.012-inches). Whenever possible, flight hardware which was supplied to Calspan by AiResearch was utilized in constructing the model. In order to minimize the flow establishment time in the test model, the approach previously [11] used for maintaining the cross-sectional area constant from the model inlet to the stator nozzle inlet and the exit area constant from the stator nozzle exit to the cylindrical section just upstream of the orifice plate was used in this design. The orifice plate is used to set the mass-flow rate through the device and thus to set the exit Mach number of the stator nozzle. This particular stator vane is designed to operate with a subsonic exit Mach number.

A photograph of one of the heat-transfer gages used in this work was taken through a Leitz microscope and is shown in Figure 3. The technology used to construct these gages has been well established for many years, as described by Vidal [23]. The Pyrex insulating substrate for the metallic film is

3

9.7 x 10^{-4}-meters (0.038-inches) in diameter by 7.1 x 10^{-4}-meters (0.028-inches) thick. The thin-film gage is made of platinum (~1000 Å thick) and is painted on the substrate in the form of a strip approximately 1.0 x 10^{-4}-meters (0.004-inches) wide by about 5.1 x 10^{-4}-meters (0.020-inches) long. The response time of these heat-transfer elements is on the order of 10^{-8} sec [23]. A coating of magnesium fluoride (~1200 Å thick) is vapor deposited over the gage to protect against abrasion. These gages are very durable in a clean environment, and a very low loss rate of gages was experienced during the measurement program. A diamond drill was used to notch the substrate on each side so as to permit the lead wires access to the thin film without shorting as a result of contact with the metal nozzle. The gages are held in the turbine components using an epoxy adhesive. They are installed under a microscope so as to ensure that they are flush with the local surface contour to within less than 1.3 x 10^{-5}-meters (0.0005-inches).

The temperature vs time histories of the thin-film gages located on the stator and the shroud were recorded directly on tape recorders with a frequency response of 20 KHz. These data were then processed through a standard analog heat-flux network (developed by Skinner [24]), and they also were analyzed using a digital version of the heat-flux equation. The results of the two analysis techniques are consistent, but the digital version allows retention of the 20 KHz frequency response.

The temperature vs time histories obtained from the heat-transfer gages located on the rotating airfoils are transferred to the previously mentioned tape recorders by use of a slip-ring system. Each heat-transfer gage is a separate circuit with the power supply for the entire array located in the tunnel control room. During the experiments, a constant current of 1 milliampere was passed through each gage (which has room temperature resistance on the order of 50 to 100 Ω) via the slip rings. The resulting i^2R heating of the gage produced less than 0.1% of the gage ΔT experienced during an experiment. The slip ring was built by Poly Scientific Corporation but the assembly and associated cooling system were purchased from CTL Dixie Corporation. The slip-ring contact noise is on the order of 25 μ volts compared to a heat-transfer gage output in the tens of millivolt range. These rotor heat-flux data were processed in the manner

4

discussed above, but the tape recorder frequency response was not sufficient to resolve the rotor-blade passage phenomena that were anticipated as the rotor blades pass through the nozzle exit passages. This particular turbine has 78 rotor blades and 41 stator passages. In order to obtain these high-frequency data, a four-channel Biomation Waveform recorder (Model 2805) with a maximum frequency response of 1.2 MHz was used to obtain temperature vs time histories from four selected gages. Two gages on the rotor and one each on the shroud and nozzle end wall were sampled. The Waveform recorder was operated so as to sample at 2μsec intervals for these selected locations with typical passage times through a stator wake being on the order of 50 to 80μsec, depending on rotor speed. A 2μsec sampling rate provided many data points during a typical blade passage.

As previously noted, this experimental program utilized a full turbine stage with the stator nozzle, the shroud, and the rotor instrumented. Figures 4 and 5 are photographs of the instrumented stator nozzle end wall and airfoil. This instrumented stator was previously used to obtain the results presented in [11]. The stator contains approximately 58 heat-transfer gages at locations[*] discussed in detail in that reference. Figures 6 - 8 are photographs of the heat-transfer gage instrumentation located in the rotor pressure surface (12 gages), suction surface (7 gages), and tip (2 gages). Figure 9 is a photograph of the heat-transfer gages and pressure transducers installed in the shroud.

Pressure transducers (PCB Model 112M and 113M) were installed in the test model from the entrance section to the orifice plate in order to obtain detailed data on the starting process and the stage performance. In addition, three Kulite (XCR-080-300A) transducers were placed at the stator exit plane in the tip end wall, and six more Kulite transducers were installed at selected axial

_____

[*]The locations selected for placement of these gages were mutually agreed upon by the AFAPL, Calspan and AiResearch. This particular stator has provision for trailing-edge cooling, but cooling gas was not utilized for the experiments discussed herein and the cooling slots were sealed.

locations in the shroud above the rotor. The Kulite transducers have a frequency response on the order of 200 KHz and the PCB transducers have a frequency response on the order of 250 KHz. The Kulites were also used to help determine flow establishment time in the rotor region and to obtain stage performance data for comparison with the AiResearch steady-state rig data.

SECTION III

EXPERIMENTAL RESULTS

Table 1 gives the experimental conditions at which heat-flux measurements were performed. The following data were obtained for corrected speeds ($N_{corr} = N_{phy}/\sqrt{T_0/513}$) ranging from approximately 70% to 106% of design corrected speed: 1) the shock-tube reflected-shock temperature and pressure, T_0 and P_0; 2) the weight flow; 3) Mach number at the start of the forward bullet nose; 4) the Mach number at the inlet to the stator nozzle/corresponding total pressure; and 5) the stator-nozzle inlet Reynolds number based on stator mid-chord, c_s . The engine idle condition is 78% corrected speed at sea level. As illustrated in Table 1, 16 separate experiments were performed. For most of the experimental conditions, approximately 90 heat-flux measurements were obtained. The different weight-flow rates were achieved by changing the model exit orifice plate shown in Figure 2. The different total temperatures were obtained by changing shock-tube conditions.

Static pressure measurements were performed at several locations along the model and in the stationary shroud in the proximity of the rotor passage. These measurements allowed the determination of flow establishment time and the pressure change across the stage. Figure 10 illustrates the character of the model pressure histories obtained on the front portion of the inlet bullet nose, on the bullet nose just upstream of the stator inlet (hub wall) and in the exit section of the model. What appears to be noise on these pressure records is presumed to be associated with the presence of the rotor. The same pressure transducers were used at similar relative locations in the stator-only experiments [22], and the pressure records have much less noise associated with them. It should also be noted that the pressure record obtained using the transducer located in the exit region is very similar to the corresponding record in the earlier experiments [22]. The early portion of the pressure record demonstrated a flow establishment time of approximately 5 to 7 milliseconds, consistent with previous results [22] and with the estimated starting time calculated using one-dimensional gas dynamics. The exit section pressure history was used in conjunction with known aft section physical dimensions and the shock-tube reservoir parameters in order to calculate the mass-flow rate at the orifice plate using isentropic relationships.

The pressure change across the turbine stage was found to be in agreement with the AiResearch rig-test results[3] over the entire speed range studied here. AiResearch measures the ratio of total pressure at stator entrance to total pressure at rotor exit to be equal to 1.45 for the 78% speed point (ground idle). The value of this ratio measured during these experiments was 1.46, which is within 1% of the steady-state rig data. Similar comparisons made at other operating conditions were within 2 to 3%.

Figures 11(a) and (b) present typical data obtained using the shroud pressure transducers for the stator exit pressure history and the pressure history near the rotor midchord. The flow establishment time within the stage is seen to be approximately three or four milliseconds more than required for the remainder of the model. The pressure fluctuations observed during the test time were time resolved on a separate oscilloscope by using a delay generator on the oscilloscope sweep.

Figure 12(a) includes the two time resolved shroud pressure histories mentioned above for the rotor mid chord and the stator exit regions. The mid-chord record shows a fluctuating pressure with a period approximately equal to the blade passage time, suggesting that the structure of the pressure history is a result of the rotor. The data shown on the lower trace of Figure 12(a) were taken from a pressure transducer located at the stator exit in the tip end wall. The magnitude of the pressure variation is of the same order as that observed from the shroud transducer in the immediate vicinity of the rotor, but the period is significantly different and the transition from pressure surface to suction surface is not as well defined. The measurement obtained at the stator exit suggests an upstream pressure influence at the tip end wall presumably because the stator vane has a subsonic exit flow. It is important to note that the magnitude of the pressure fluctuation $\sim$124 kPa (18 psi) is consistent with results obtained at this condition by AiResearch for this particular turbine. Similar agreement was achieved at other operating conditions.

---

[3] T.C. Booth, AiResearch Corporation, Phoenix, Arizona, private communication to M. G. Dunn, October 1980.

A gallium arsenide infrared emitting diode and a silicon npn photo-transistor array (referred to herein as a light emitting diode) were located just behind the rotor which had the trailing edge of every 13th blade painted white. The reflection from the white blade was so much greater than that from the adjoining unpainted blades that the LED could be used to provide a measure of the rotor speed from which the rotor-blade period could be calculated. A typical LED history is presented in Figure 12(b). The unpainted blades can be seen as sub-structure on the record, but the white blades are obvious. For the case shown in Figure 12(b), the average time between painted blades, τ_1, was approximately 415 μ sec. Since there are 78 blades on the rotor, and one obtains 6 pulses every rotor revolution. the rotor speed can be shown to be equal to RPM = $10/\tau_1$. Knowing the rotor speed and the total number of blades on the rotor, the time between successive blade passages at a fixed point on the shroud, τ_2, was calculated to be approximately 32 μ sec for the case given in Figure 12(b).

The heat-flux data obtained in these experiments has been used to obtain plots of Stanton number, St = $\dot{q}A/\dot{m}(H_o-H_w)$, vs Reynolds number based on mid-annular stator chord, $\rho V c_s/\mu$. The Stanton number is obtained from the measured heat flux, $\dot{q}$, the stator inlet area, A, the mass flow rate, $\dot{m}$, and the known enthalpy difference, H_o-H_w. The Reynolds number is obtained by dividing the mass-flow rate by the stator inlet area, A, to obtain the quantity ρV, while the mid-annular stator chord, c_s, is known, and the viscosity, μ, can be evaluated at the total enthalpy, H_o. The previous stator-only data [11] for the same stator stage have been cast in the same format for the purpose of comparing those results with the full-stage results.

Figure 13 presents the data obtained for four specific gages on the stator tip end wall, two near the entrance to the passage (gages #33 and #34) and two further along in the channel (gages #45 and #46). The heat-flux gages selected for comparison in this discussion were chosen to be representative of the data. For comparison purposes, the previous stator-only data are included on this figure and those that follow. With the exception of the stator-only data of gage #33, the results obtained with or without the rotor are in good agreement. The stator-only data for gage #33 is the only end wall

9

gage that deviated significantly from the corresponding full-stage data. The data presented on Figure 13 suggest that the end-wall Stanton number is independent of Reynolds number and corrected speed over the range of those parameters investigated.

A similar plot is presented in Figure 14 for gages located near the stator airfoil leading edge. The stator-only data of gages #5 and #3 are in reasonably good agreement with the full-stage data, but the gage #19 stator-only heat flux is lower. In general, the stator-only data obtained on the suction surface near the leading edge from gage #19 towards the tip end wall were consistent in that they were significantly lower than the full-stage data. By comparison, the results for gages located closer to the hub end wall were more consistent with the pressure surface result shown on Figure 14 in that the stator-only data are within 15% of the full-stage results.

Data obtained for the aft portion of the airfoil are presented in Figure 15 for both the suction and pressure surfaces. The suction surface results suggest an increasing Stanton number with increasing Reynolds number, perhaps indicating boundary-layer transition. A later plot (Figure 18) compares the pressure surface and suction surface Stanton numbers as a function of chord position. The pressure surface data appear to be independent of both Reynolds number and corrected speed. The stator-only data were on the order of 20% below the full-stage data.

The data presented in Figures 13-15 were also plotted as a function of % corrected speed. The stator-tip end-wall data are given on Figure 16. These results suggest that the end-wall heat-flux values at selected locations are independent of rotor speed. With the exception of a single data point at 96% corrected speed, essentially the same result is illustrated in Figure 17 for the stator airfoil pressure surface. However, the data shown in Figure 17 for the airfoil suction surface illustrate a somewhat different trend in that the heat-flux increases with increasing corrected speed.

10

The data discussed above were also cast into a distribution of Stanton number over the airfoil and the result is presented in Figure 18 and compared to the stator-only result. Note that the Reynolds numbers for these two sets of data are slightly different. The 70% corrected speed data were selected for this comparison because of the comparable Reynolds numbers. The general shape of the distribution is qualitatively the same for both the stator-only experiments and the full-stage data, and is consistent with the distributions measured for a rotor blade by Martin, et al. [25]. Evidence of boundary-layer transition can be seen near the 25% chord position on the suction surface. Once again, the stator-only data appear to indicate lower Stanton numbers than the corresponding full-stage data.

Heat-flux results for the rotor shroud and tip are presented in Figure 19 and a typical raw data record for the shroud region is given in Figure 20. The shroud region Stanton numbers are presented as a function of mid-annular rotor chord position, % of c_r . These data, which were obtained from approximately 22% to 90% of the rotor chord, suggest that the Stanton number is relatively constant in the axial direction along the shroud. The results also suggest that at a given location, the effect of rotor speed appears to be an increase in the heat flux. However, it should be noted that at the higher speed, the Reynolds numbers are also higher, so that what is observed is possibly a Reynolds number effect. In addition, the tip data presented on Figure 19 indicate that the tip heat-flux values are somewhat greater than the shroud values, and also increase with increasing Reynolds numbers.

The shroud and tip regions were found to be the regions of highest heat-flux in the turbine. For comparison purposes, one of the rotor suction surface measurements is presented in Figure 21 and a typical rotor pressure surface measurement is presented in Figure 22. The resulting Stanton numbers for the blade surfaces are about 60% to 70% of the corresponding shroud value. These figures include typical heat-flux history records obtained from the analog network [24]. The fluctuations appearing on the heat-flux record of Figures 21 and 22 are indicative of the flow environment and gage noise. The heat-flux measurements, for nominally the same flow conditions, are repeatable to within approximately ±5%. Note that the results presented in Figures 13 - 19 were

obtained at actual rotor speeds that were within ±3% of the nominal rotor speeds. The flow establishment time is noted on this record and is consistent with the values shown on the earlier shroud region pressure histories.

As noted earlier, a Biomation waveform recorder was used to record high frequency response information (on the order of 1 megahertz) for selected portions of the turbine stage. A heat-flux analog of comparable frequency response was not available. Therefore, the recorder was used to record the temperature-time histories of these selected heat-flux gages. A typical example of the results obtained for a gage on the stator tip end wall near the rotor face and for a gage located on the rotor suction surface are shown in Figure 23(a) and (b). For this particular experiment, the rotor passage time through a stator wake was on the order of $73\,\mu$sec and the gage output was sampled every $2\,\mu$sec. Figure 23(a) suggests a large spike in heat-flux at the stator end wall gage that corresponds to the frequency of rotor passage through the stator wake. Figure 23 (b) illustrates a minimal influence of the stator wake on the rotor blade temperature history.

SECTION IV

CONCLUSIONS

Detailed heat-flux and pressure data have been obtained for the full-stage AiResearch TFE 731-2 turbine using state of the art shock-tube technology and transient-test techniques. The stage pressure data obtained in these experiments were found to be in good agreement with the steady-stage rig data obtained by AiResearch for this turbine. Comparisons are presented between the previous Calspan experiment with the TFE 731-2 stator-stage only and the current full-stage data. The stator end-wall Stanton number appears to be independent of stator-stage only or full-stage configuration, Reynolds number and corrected speed. The full-stage stator airfoil data demonstrate a significant influence of the presence of the rotor at comparable Reynolds numbers, suggesting that caution should be exercised when applying stator-only results to full-stage predictions. For this turbine, the stator-only Stanton numbers for the stator airfoil are shown to be approximately 20% less than the corresponding full-stage results. The shroud heat flux was found to be independent of rotor chord position, but increased with increasing Reynolds number. The tip heat flux was found to be somewhat greater than the shroud heat flux and it also increased with Reynolds number.

REFERENCES

1. Project SQUID Workshop on Cooling Problems in Aircraft Gas Turbines, Naval Postgraduate School, Monterey, California, 27-28 Sept. 1978.

2. Gas Turbine Heat Transfer and Cooling Technology - Current Status and Future Needs, Panel Discussion, 25th Annual International Gas Turbine Conference, New Orleans, La., 9-13 March 1980.

3. Workshop on Fundamental Heat Transfer Research for Gas Turbine Engines, NASA-Lewis Research Center, 8-9 October 1980.

4. Dodge, P.R., "Numerical Method for 2D and 3D Viscous Flows", AIAA Journal, Vol. 15, July 1977, pp. 961-965

5. Katsanis, T., "Fortran Program for Calculating Transonic Velocities on a Blade-to-Blade Stream Surface of a Turbomachine", NASA Tech. Note D-5427, September 1969.

6. Wu, C.H., "A General Theory of Three-Dimensional Flow With Subsonic and Supersonic Velocity in Turbomachines Having Arbitrary Hub and Casing Shapes - Parts I and II", ASME Paper 50-A-79, 1950.

7. Smith, L.H., "Radial Equilibrium Equations of Turbomachinery", ASME 65-WA/GTP-1, 1965.

8. Horlock, J.H., and Perkins, H.J., "Annulus Wall Boundary Layers in Turbomachines", AGARD-AG-185, 1974.

9. Booth, T.C., "An Analysis of the Turbine Endwall Boundary Layer and Aerodynamic Losses", ASME Paper 75-GT-23, ASME Gas Turbine Conference, Houston, Texas, March 2-6, 1975.

10. Dodge, P.R., "3-D Heat Transfer Analysis Program", Final Technical Report AFAPL-TR-77-64, October 1977.

11. Dunn, M.G., and Stoddard, F.J., "Measurement of Heat-Transfer Rate to a Gas Turbine Stator", J. Engineering for Power, Vol. 101, No. 2, April 1979.

12. Blair, M.F., "An Experimental Study of Heat Transfer and Film Cooling on Large-Scale Turbine Endwalls", ASME Journal of Heat Transfer, Vol. 96, Nov. 1974, pp. 524-529.

13. Graziani, R.A., Blair, M.F., Taylor, J.R., and Mayle, R.E., "An Experimental Study of Endwall and Airfoil Surface Heat Transfer in a Large Scale Turbine Blade Cascade", J. of Engineering for Power, Vol. 102, pp. 257-267, April 1980.

14. York, R.E., "Experimental Investigation of Turbine Endwall Heat Transfer", Detroit Diesel Allison, Final Report in preparation.

15. Dring, R.P., Blair, M.F., and Joslyn, H.D., "An Experimental Investigation of Film Cooling on a Turbine Rotor Blade", J. of Engineering for Power, Vol. 102, pp. 81-87, January 1980.

16. Louis, J.F., "Investigation of Factors Affecting Heat Transfer to Turbine End Walls", Air Force Aero-Propulsion Laboratory, TR-73-93, October 1973.

17. Louis, J.F., "Heat Transfer in Turbines", Air Force Aero-Propulsion Laboratory, TR-75-107, September 1975.

18. Jones, T.V., and Schultz, D.L., "A Study of Film Cooling Related to Gas Turbines Using Transient Techniques", University of Oxford Report No. 1121/70, 1970.

19. Jones, T.V., Schultz, D.L., Oldfield, M.L.G. and Daniels, L.C., "Measurement of the Heat Transfer Rate to Turbine Blades and NGV's in a Transient Cascade", 6th International Heat Transfer Conference, Toronto, Canada, Paper EC-12, 1978.

20. Schultz, D.L., Jones, T.V., Oldfield, M.L.G., and Daniels, L.C., "A New Transient Facility for the Measurement of Heat Transfer Rates", Conference Proceedings No. 229, High Temperature Problems in Gas Turbine Engines, pp. 31-1 to 31-27, September 1977.

21. Smith, M.R., "A Study of Film Cooling Effectiveness with Discrete Holes and Slots", University of Oxford Report No. 1100/74, 1974.

22. Dunn, M.G., and Stoddard, F.J., "Development of a Shock-Tunnel Technique for the Measurement of Heat-Transfer Rate to Gas Turbine Components", 11th International Symposium on Shock Tubes and Waves, July 1977.

23. Vidal, R.J., "Model Instrumentation Techniques for Heat Transfer and Force Measurements in a Hypersonic Shock Tunnel", Cornell Aeronautical Laboratory Rept. No. AD-917-A-1, Feb. 1956, also WADC TN 56-315, AD97238.

24. Skinner, G.T., "Analog Network to Convert Surface Temperature to Heat Flux", Cornell Aeronautical Laboratory Rept. No. CAL-100, Feb. 1960; also American Rocket Society Journal, Vol. 30, No. 6, June 1960, pp. 569-570.

25. Martin, B.W., Brown, A., and Garrett, S.E., "Heat Transfer to a PVD Rotor Blade at High Subsonic Passage Throat Mach Numbers", AGARD Conference Proceedings No. 229, High Temperature Problems in Gas Turbine Engines, pp. 32-1 to 32-12, September 1977.

15

TABLE 1

EXPERIMENTAL CONDITIONS FOR HEAT-TRANSFER MEASUREMENTS

RUN No.	T_o °R	(Shock Tube) P_o psia	N_{phy} rpm	%N_{corr} -	M) Start of Bullet Nose	$\dot{m}$ lb/sec	P_T) Stator Inlet psia	M) Stator Inlet -	$R_E)_{c_s}$ -
1	2970	1980	20,000	68	0.15	21.4	181	0.15	1.67×10^5
2	2970	1960	20,000	68	0.15	21.4	179	0.15	1.67×10^5
3	2970	1960	20,000	68	0.14	20.6	183	0.14	1.61×10^5
4	2580	1650	20,000	73	0.16	20.2	159	0.15	1.72×10^5
5	2600	1690	20,800	76	0.16	19.7	155	0.15	1.66×10^5
6	2710	1820	21,740	78	0.15	19.7	166	0.14	1.62×10^5
7	1370	1130	21,140	106	0.16	19.3	103	0.16	2.76×10^5
8	1600	1650	22,730	106	0.16	26.1	153	0.16	2.96×10^5
9	1600	1640	26,320	122	0.16	25.9	153	0.16	2.94×10^5
10	1620	1660	22,220	103	0.16	24.6	150	0.15	2.77×10^5
11	1620	1650	20,830	96	0.18	27.6	152	0.17	3.11×10^5
12	1620	1670	22,220	103	0.17	27.1	153	0.16	3.05×10^5
13	2620	1700	21,280	77	0.19	23.2	159	0.17	1.94×10^5
14	2620	1700	24,100	88	0.18	22.8	162	0.17	1.91×10^5
15	1620	1660	0	0	-	29.7	149	0.19	3.34×10^5
16	1600	1620	0	0	0.18	27.5	145	0.18	3.17×10^5

Evacuated Dump Tank ——— 12.19 (40) ————

1.22 (4)

10.5°

0.20 (0.67)

Diaphragms

Driven

50'

15.24 (50)

Driver

40'

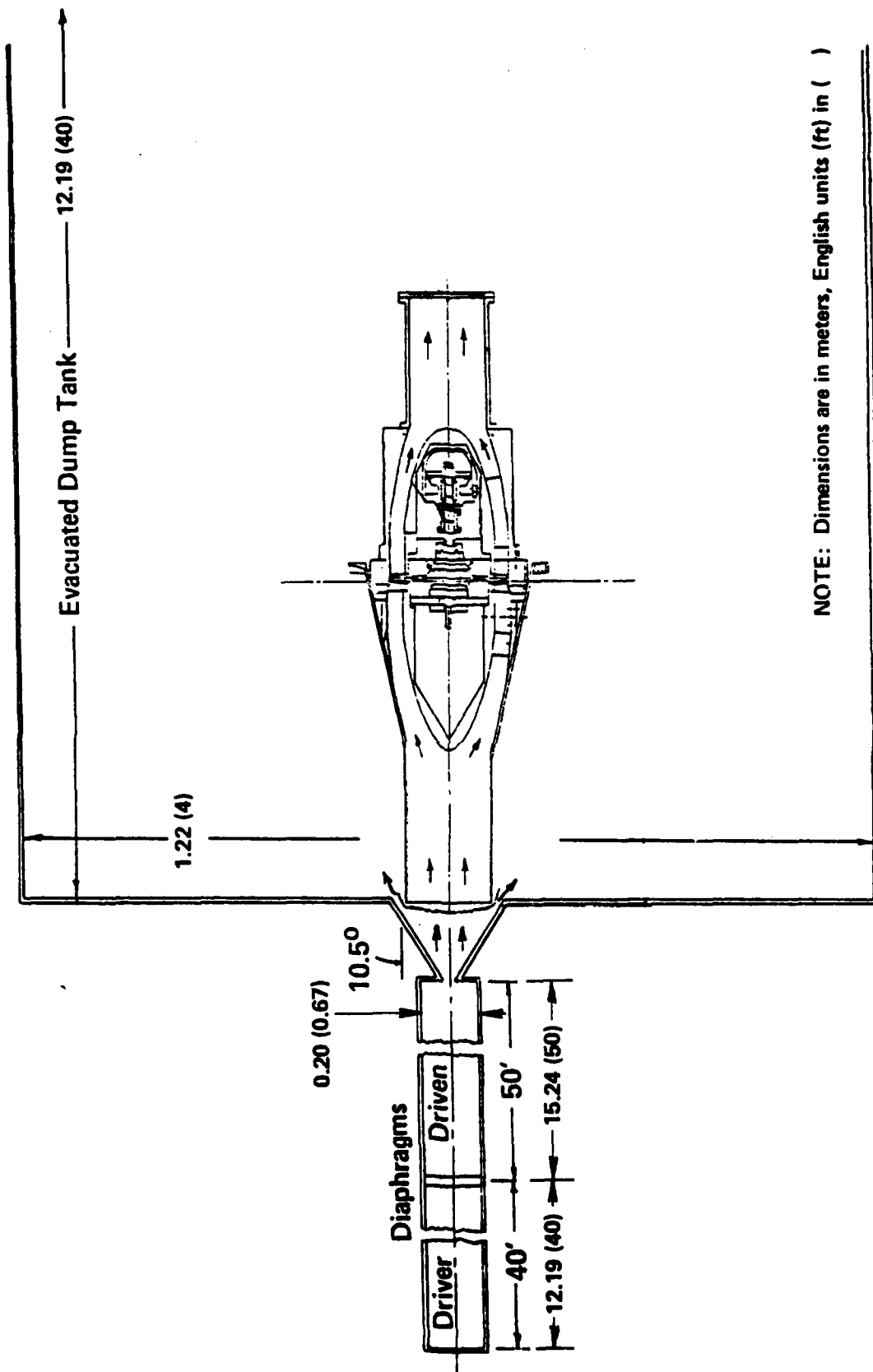12.19 (40)

NOTE: Dimensions are in meters, English units (ft) in ( )

Figure 1   SCHEMATIC OF EXPERIMENTAL APPARATUS

17
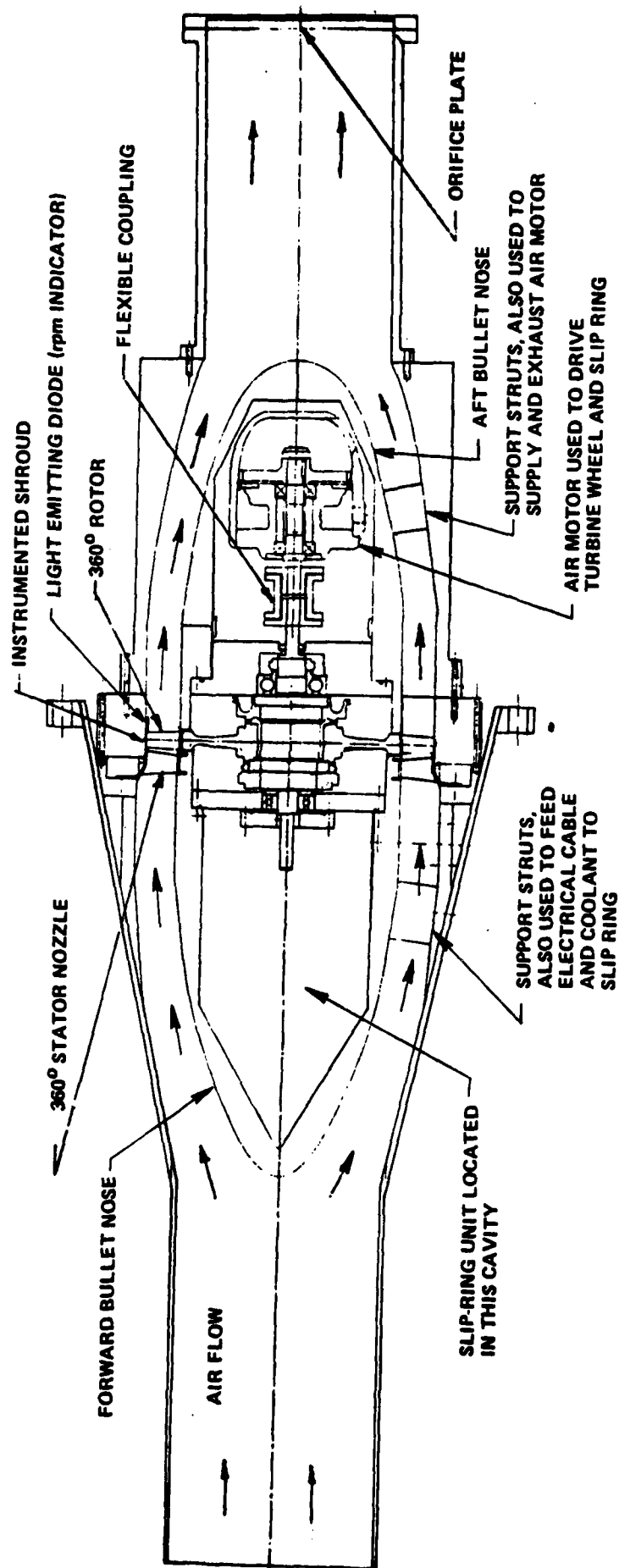
Figure 2 SCHEMATIC OF TEST-SECTION APPARATUS FOR FULL-STAGE TURBINE EXPERIMENTS

INSTRUMENTED SHROUD

LIGHT EMITTING DIODE (rpm INDICATOR)

FLEXIBLE COUPLING

360° ROTOR

ORIFICE PLATE

AFT BULLET NOSE

SUPPORT STRUTS, ALSO USED TO SUPPLY AND EXHAUST AIR MOTOR

AIR MOTOR USED TO DRIVE TURBINE WHEEL AND SLIP RING

SUPPORT STRUTS, ALSO USED TO FEED ELECTRICAL CABLE AND COOLANT TO SLIP RING

360° STATOR NOZZLE

FORWARD BULLET NOSE

SLIP-RING UNIT LOCATED IN THIS CAVITY

AIR FLOW

Figure 3 PHOTOGRAPH OF HEAT-TRANSFER GAGE TAKEN THROUGH
LEITZ MICROSCOPE

19
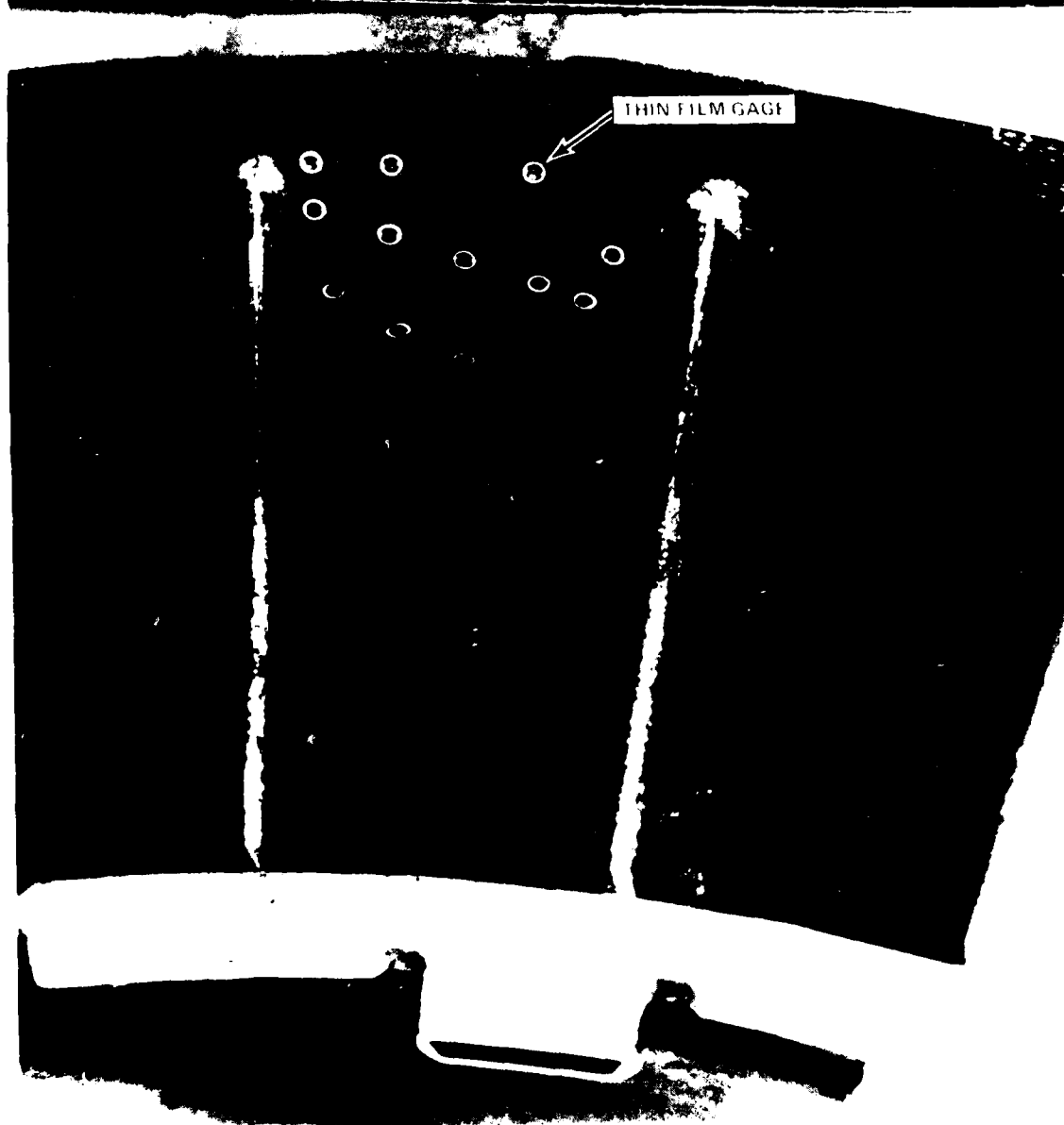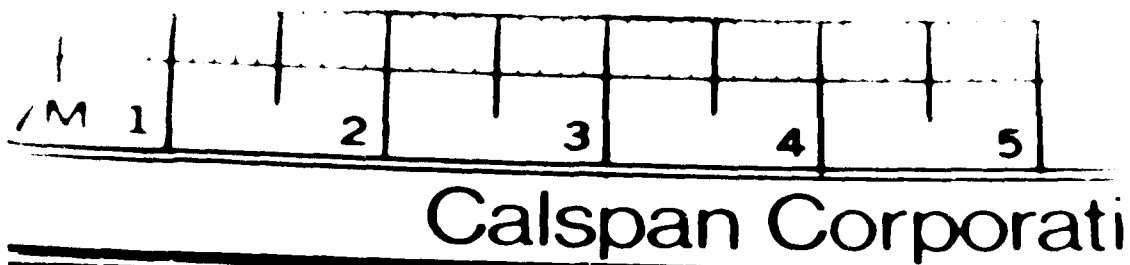
Figure 4 PHOTOGRAPH OF STATOR NOZZLE INLET

THIN FILM GAGE
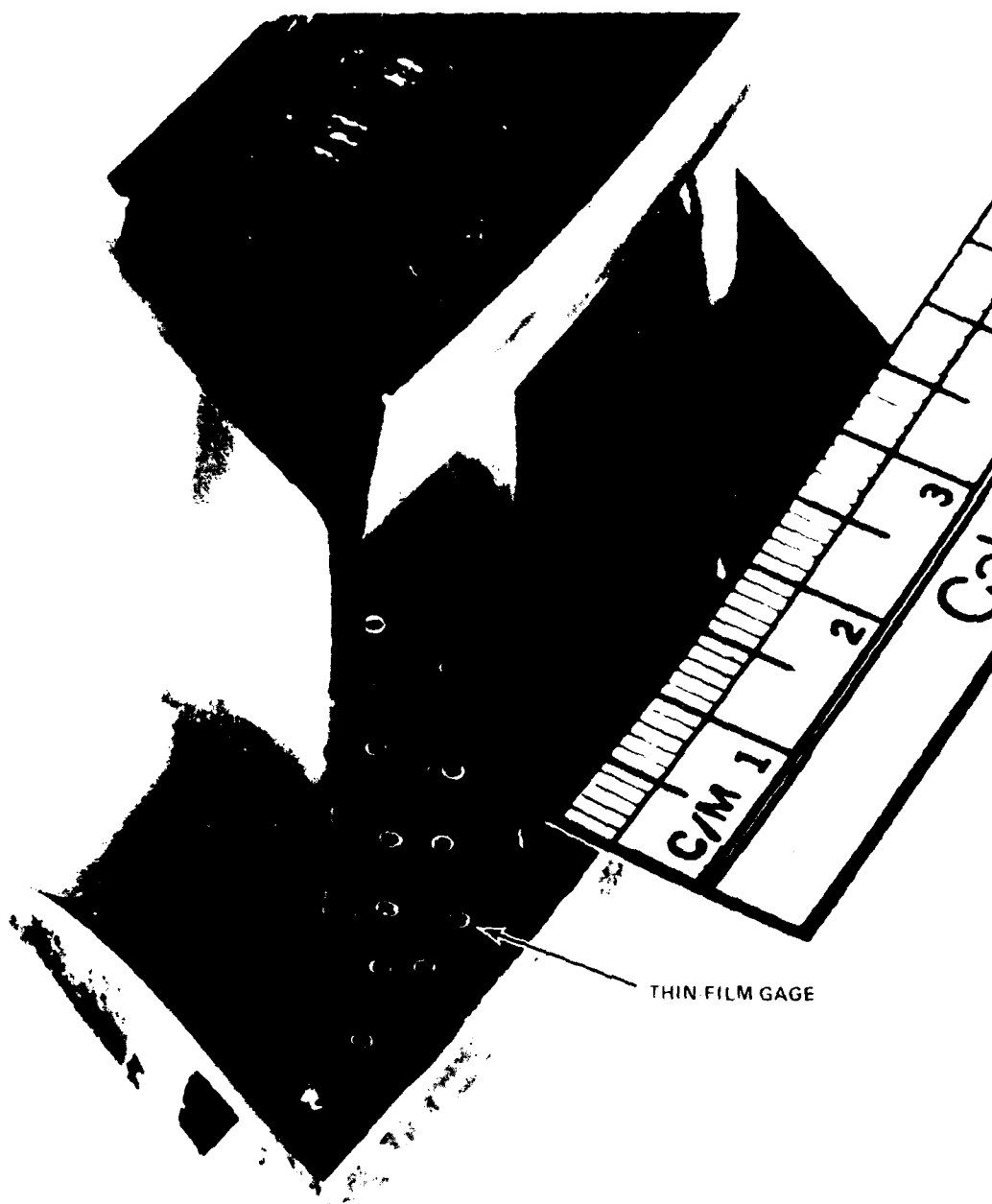
Figure 5   PHOTOGRAPH OF STATOR NOZZLE END WALL

21
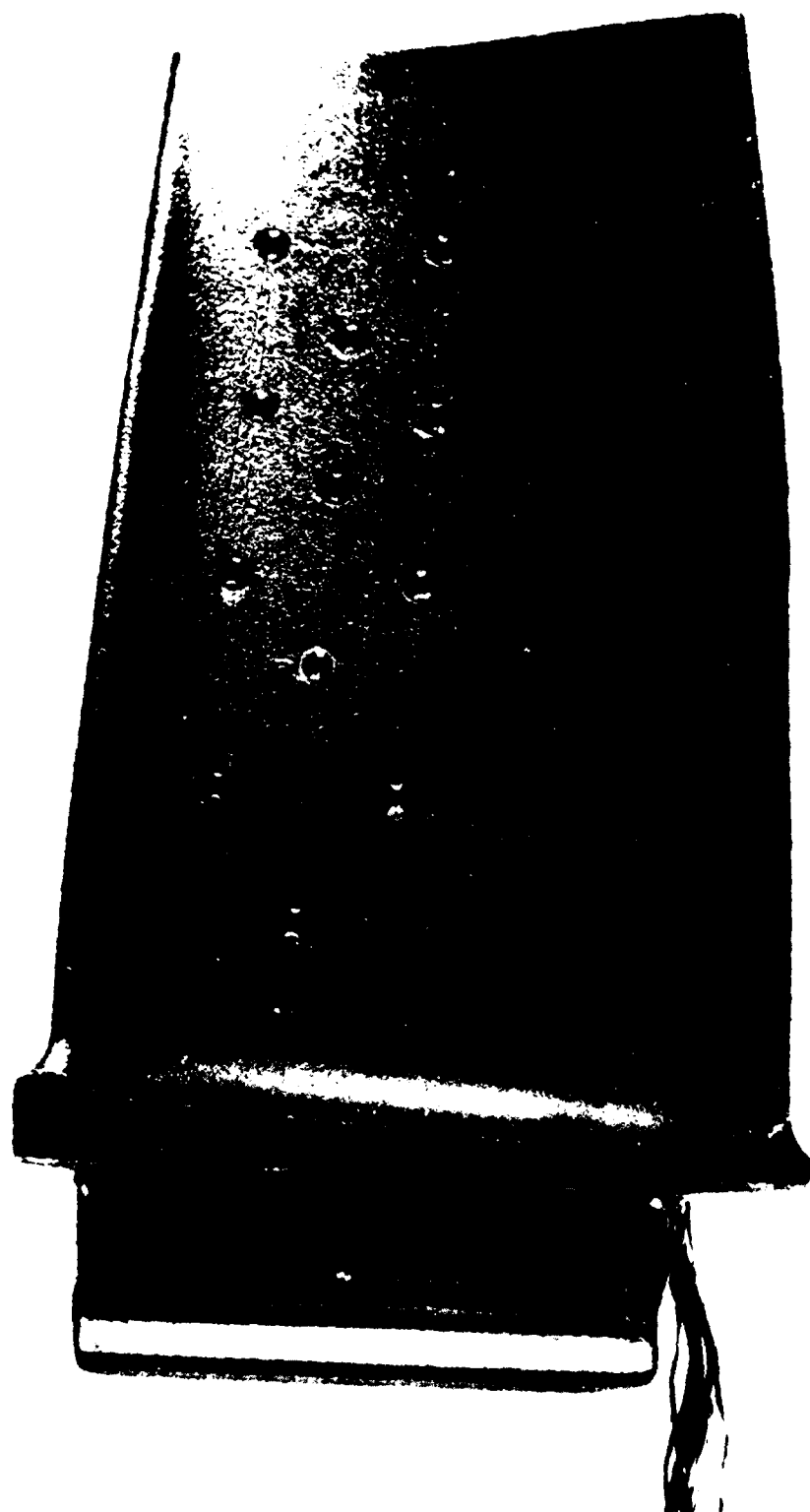
Figure 6   HEAT-TRANSFER GAGES IN ROTOR AIRFOIL PRESSURE SURFACE
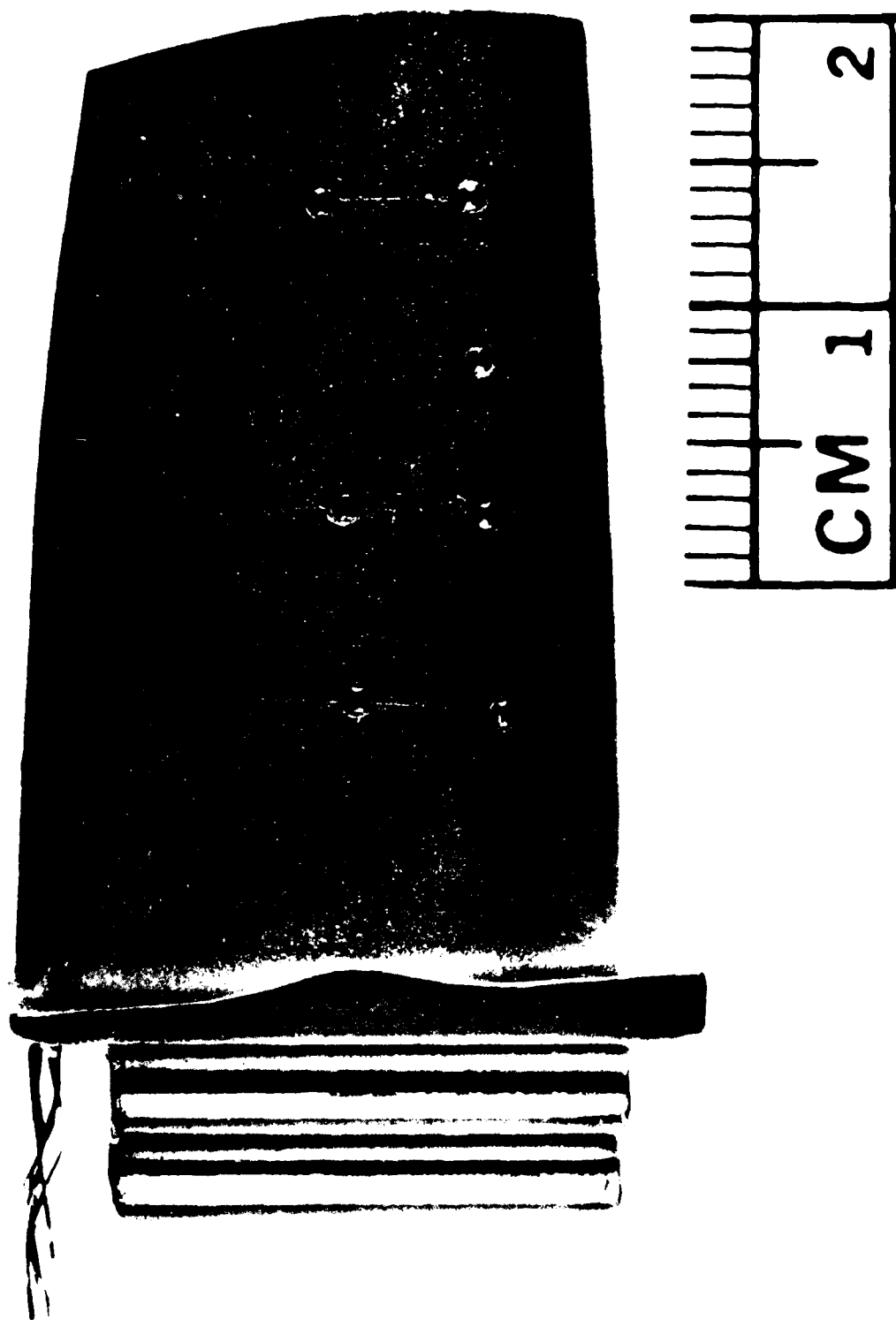
Figure 7   HEAT-TRANSFER GAGES IN ROTOR AIRFOIL SUCTION SURFACE

Figure 8   HEAT-TRANSFER GAGES IN ROTOR AIRFOIL TIP
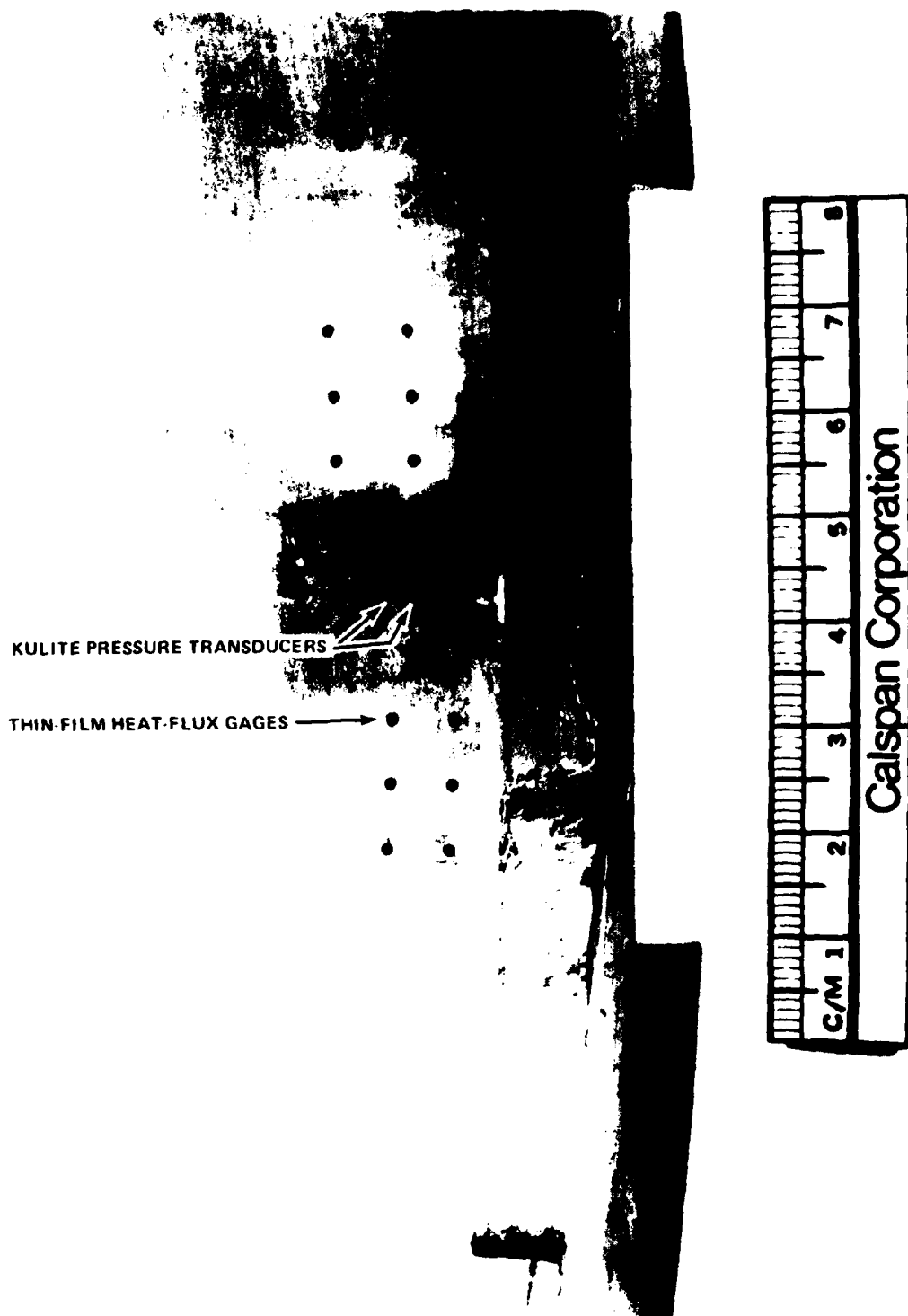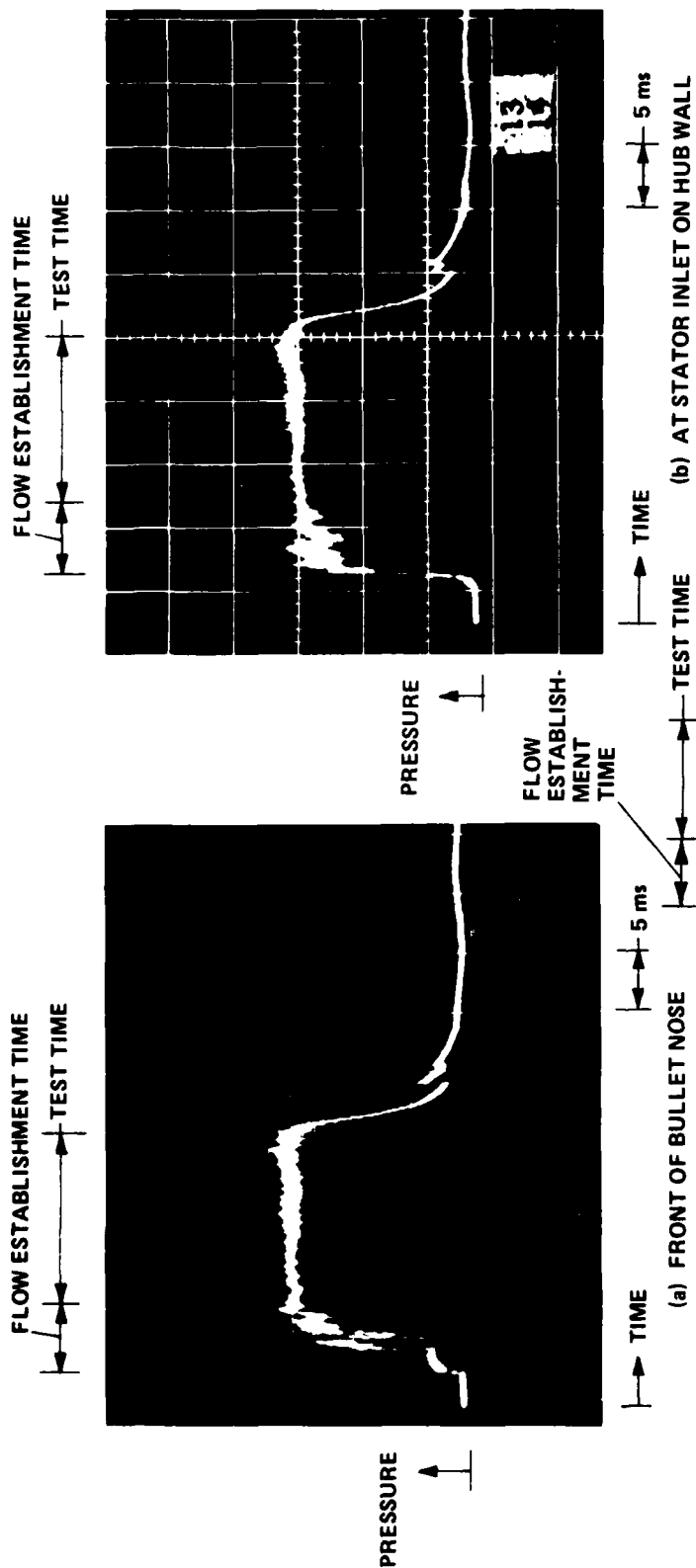
Figure 9 PHOTOGRAPH OF SHROUD HEAT-FLUX GAGES AND PRESSURE TRANSDUCER LOCATIONS

25

FLOW ESTABLISHMENT TIME

TEST TIME

PRESSURE

TIME

(a) FRONT OF BULLET NOSE

5 ms

FLOW ESTABLISHMENT TIME

TEST TIME

PRESSURE

TIME

(b) AT STATOR INLET ON HUB WALL

5 ms

FLOW ESTABLISH- MENT TIME

TEST TIME

PRESSURE

TIME

(c) IN EXIT SECTION OF TEST MODEL

5 ms

T_0 = 920°K
Re_{c_s} = 2.8 x 10^5
N_{phy} = 22,220 rpm
N_{corr} = 103%
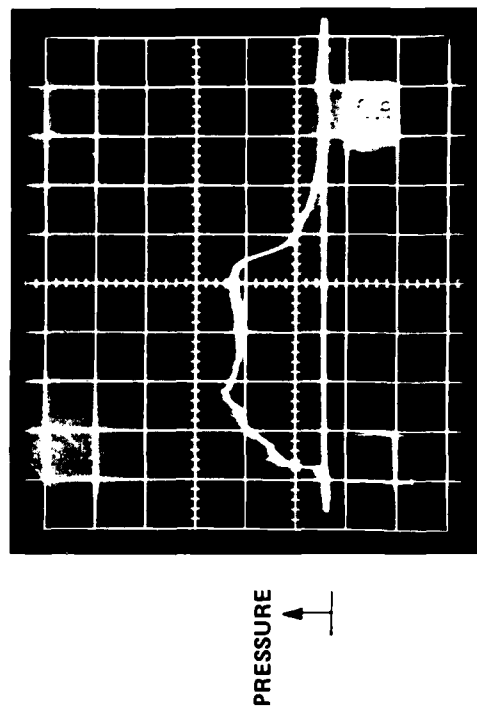
Figure 10   MODEL PRESSURE HISTORIES

26

FLOW ESTABLISHMENT TIME

TEST TIME

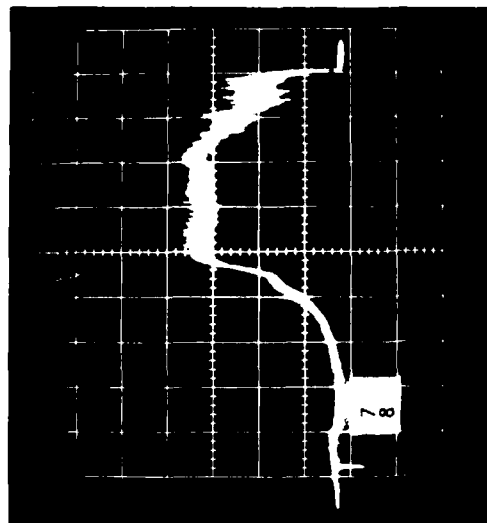PRESSURE

TIME

5 ms

(b) NEAR ROTOR MIDCHORD

FLOW ESTABLISHMENT TIME

TEST TIME
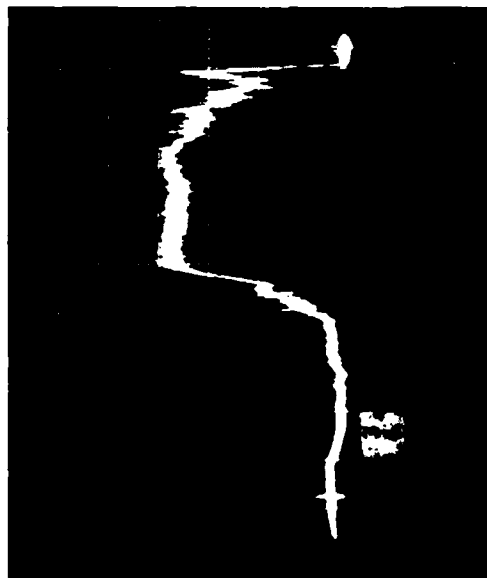
PRESSURE

TIME

5 ms

(a) AT STATOR EXIT

T_0 = 920°K
Re_{c_s} = 2.8 x 10^5
N_{phy} = 22,220 rpm
N_{corr} = 103%

Figure 11 SHROUD PRESSURE HISTORIES NEAR ROTOR

27

T_0 = 1456°K
Re_{c_s} = 1.9×10^5

200 μsec

τ_1 = 415 μsec

124 kPa (18 psi)

124 kPa (18 psi)

31 μsec
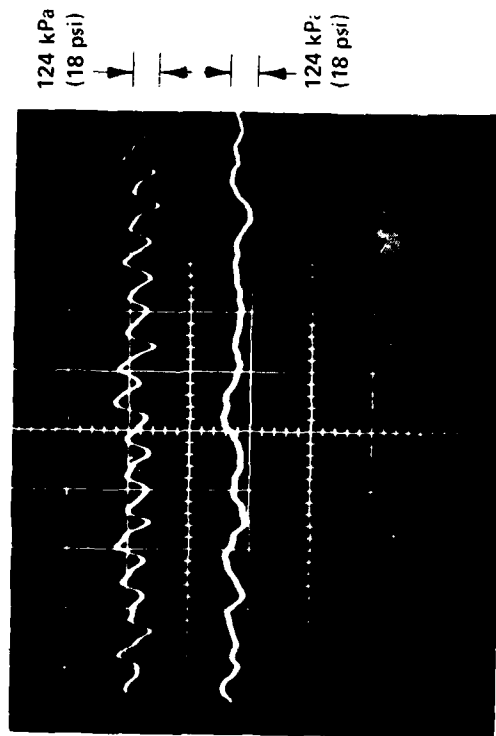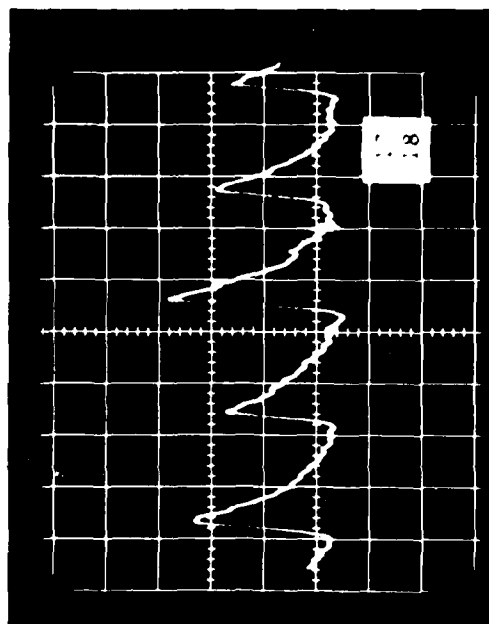
(a) UPPER TRACE, PRESSURE NEAR ROTOR MIDCHORD
LOWER TRACE, PRESSURE AT STATOR TIP EXIT

TOTAL OF 78 ROTOR BLADES
TIME BETWEEN PASSAGE OF SUCCESSIVE
BLADES DETERMINED FROM RPM

∴ τ_2 = 31.9 μsec

TIME

(b) OUTPUT OF LIGHT EMITTING DIODE
TIME BETWEEN PAINTED BLADES = τ_1
EVERY THIRTEENTH BLADE TRAILING EDGE IS
PAINTED WHITE

∴ RPM = $\dfrac{10}{\tau_1}$ = 24,100

TIME

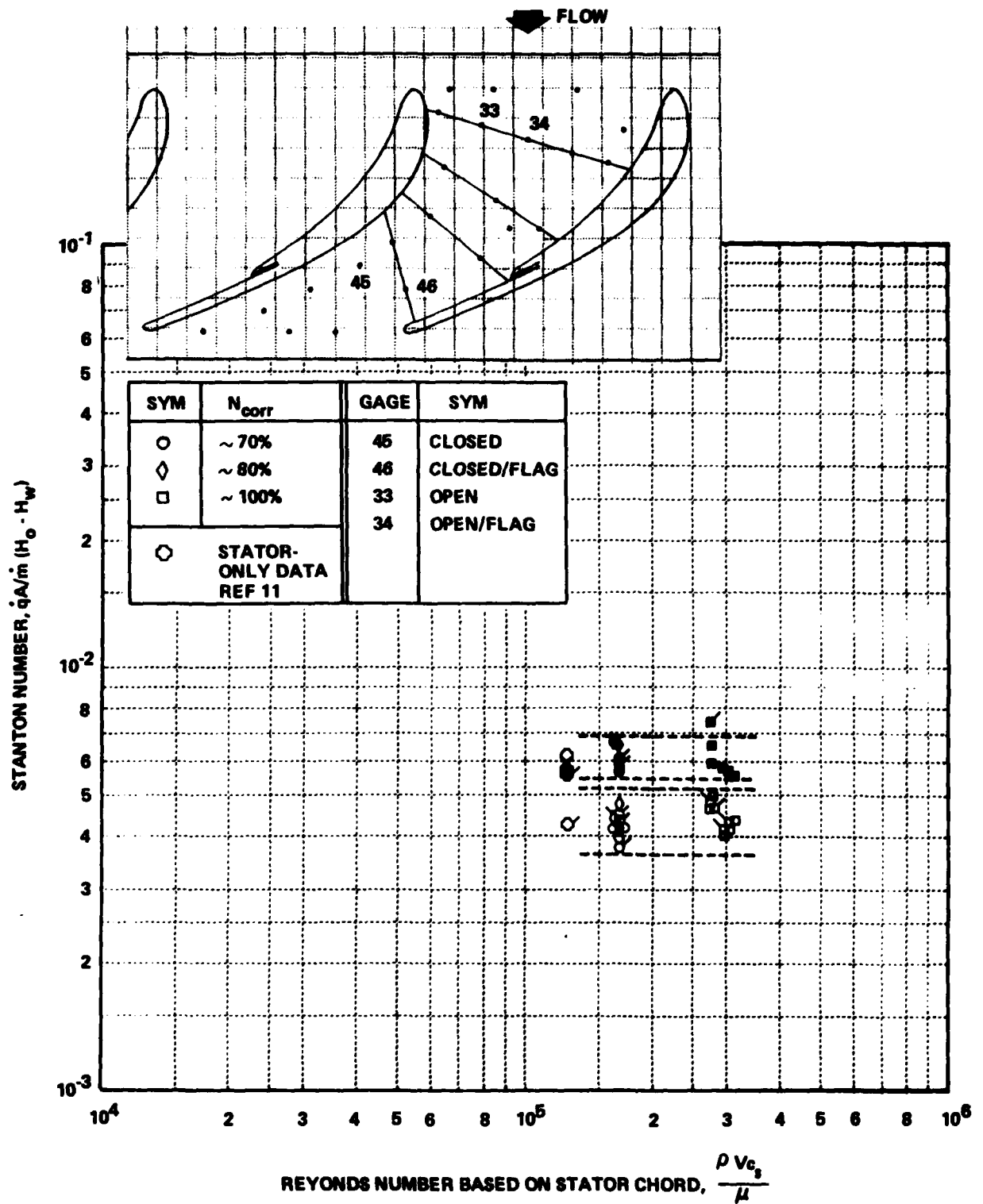Figure 12   TIME-RESOLVED SHROUD PRESSURE HISTORY AND ROTOR SPEED

28

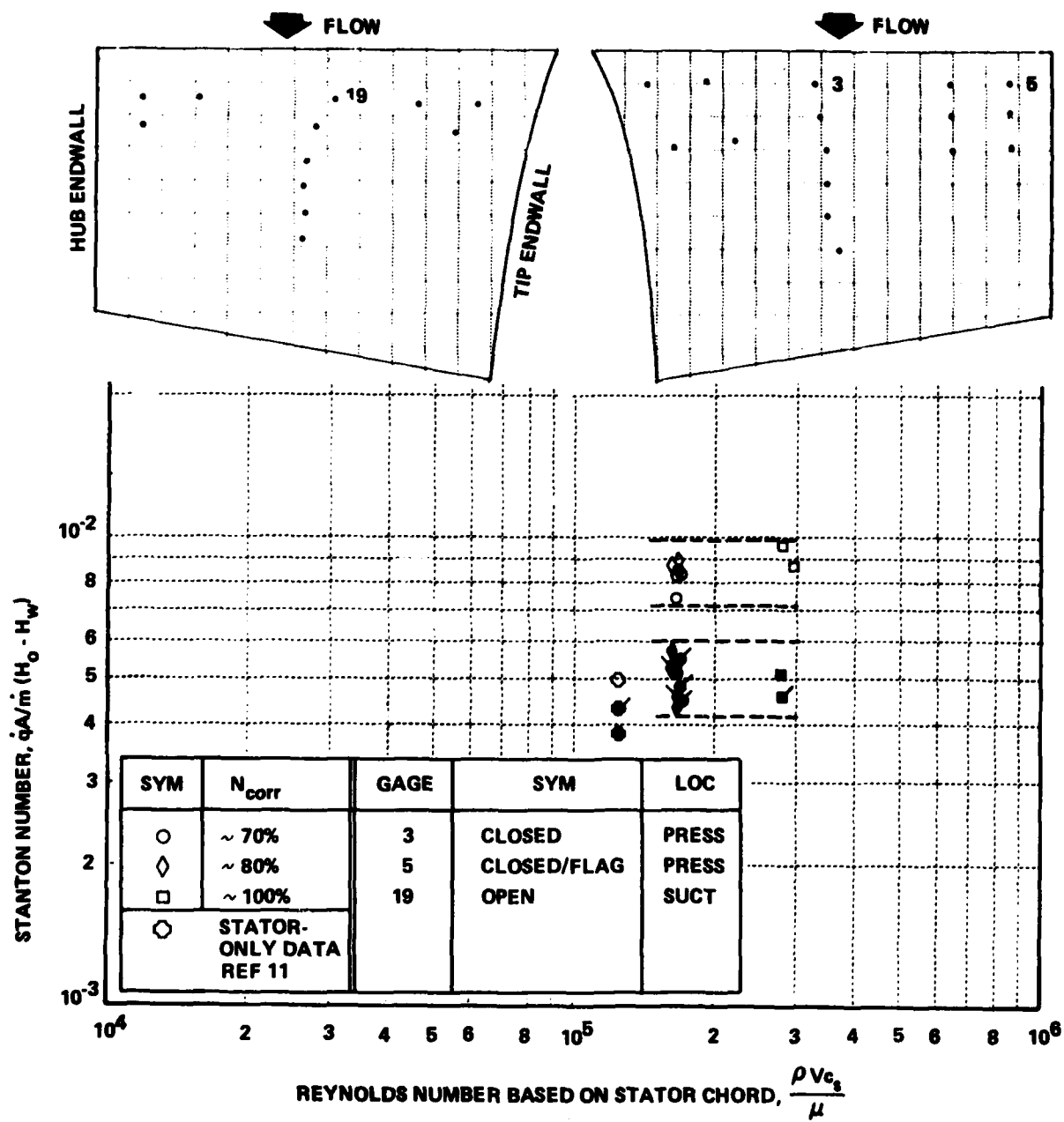Figure 13 HEAT TRANSFER TO STATOR TIP END WALL

29

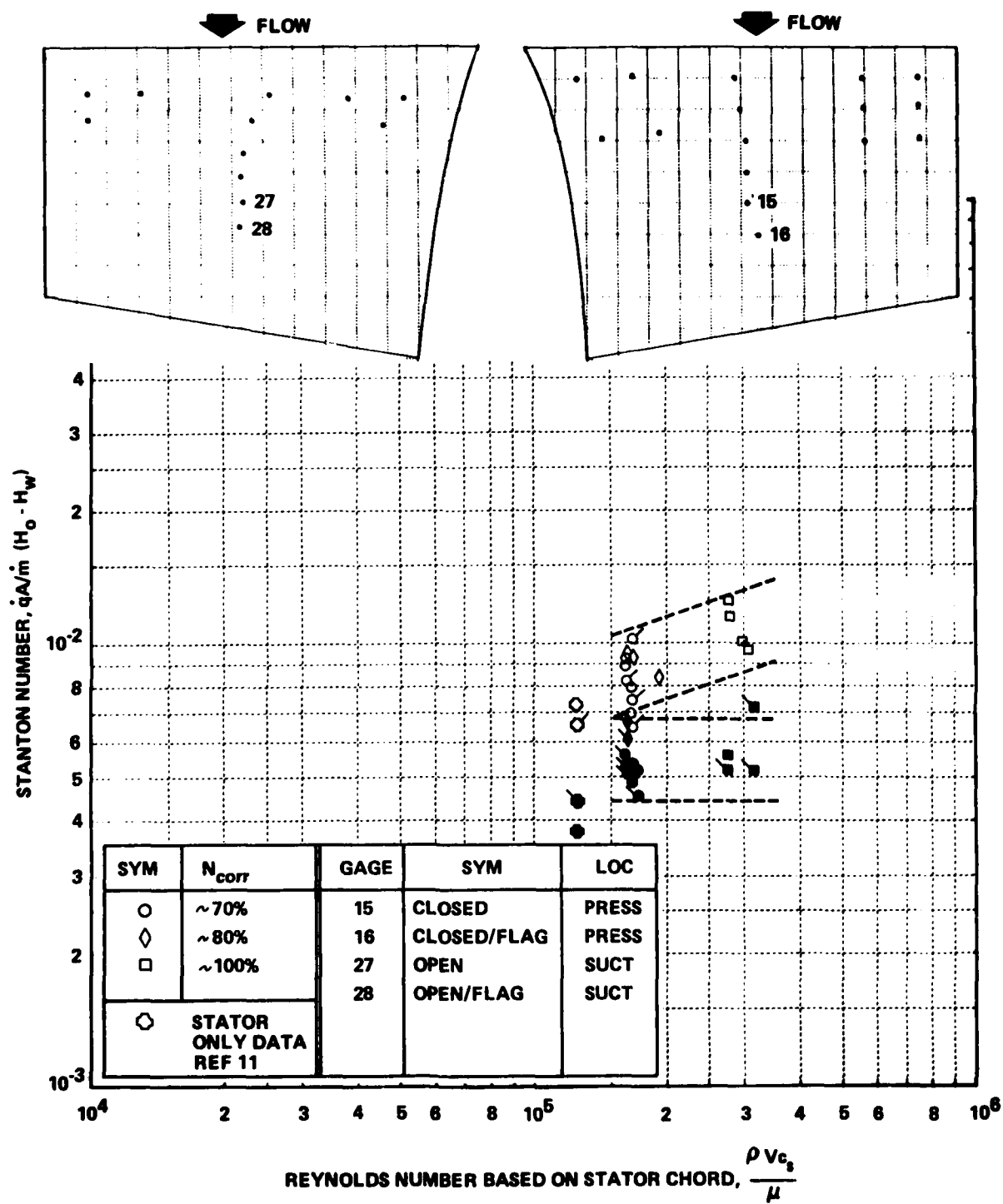Figure 14 HEAT TRANSFER NEAR STATOR AIRFOIL LEADING EDGE

FLOW

FLOW

• 27
• 28

• 15
• 16

Figure 15   HEAT TRANSFER AFT OF STATOR MIDCHORD

SYM	N_{corr}	GAGE	SYM	LOC
○	~70%	15	CLOSED	PRESS
◇	~80%	16	CLOSED/FLAG	PRESS
□	~100%	27	OPEN	SUCT
⬡	STATOR ONLY DATA REF 11	28	OPEN/FLAG	SUCT

STANTON NUMBER, $\dot{q}A/\dot{m}\,(H_o - H_w)$

REYNOLDS NUMBER BASED ON STATOR CHORD, $\dfrac{\rho V c_s}{\mu}$

31

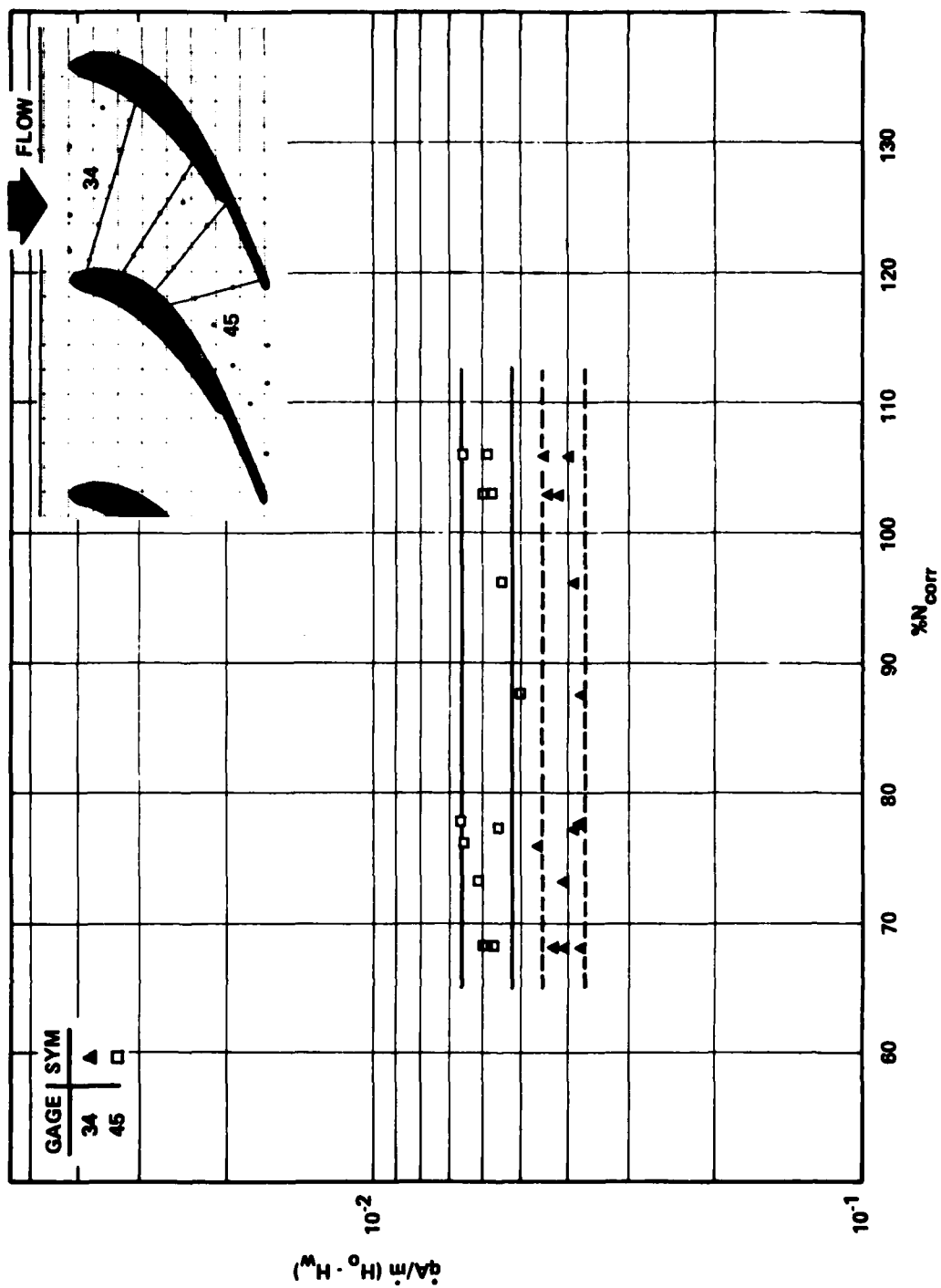Figure 16   HEAT TRANSFER TO STATOR END WALL vs CORRECTED SPEED

32
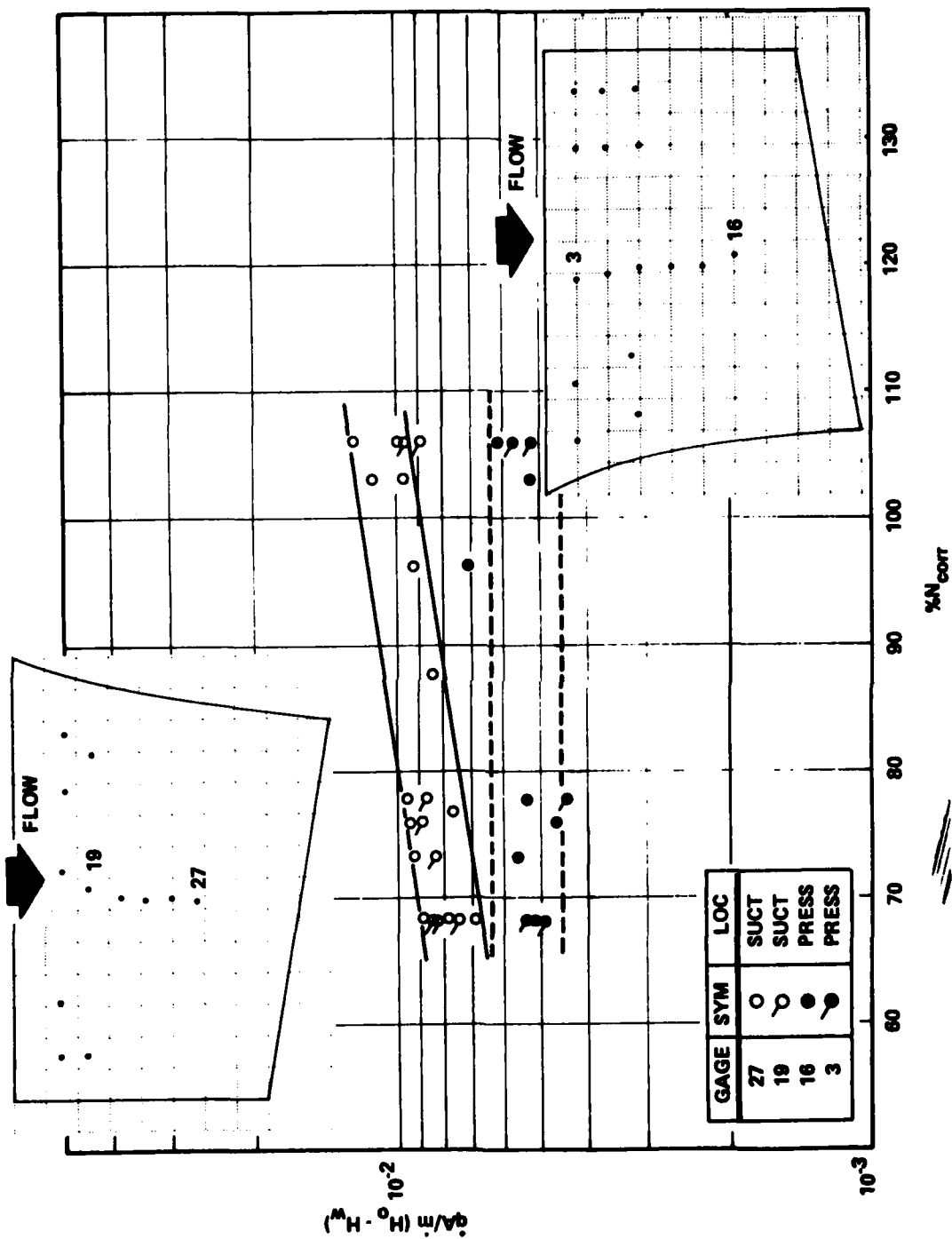
Figure 17   HEAT TRANSFER TO STATOR AIRFOIL vs CORRECTED SPEED

33

SYM	LOCATION	Re_{c_s}
○	PRESSURE SURFACE, ~70% = N_{corr}	1.67×10^5
●	SUCTION SURFACE, ~70% = N_{corr}	1.67×10^5
♂	PRESSURE SURFACE, STATOR-ONLY, REF 11	1.25×10^5
♂ (filled)	SUCTION SURFACE, STATOR-ONLY, REF 11	1.25×10^5

STANTON NUMBER

70 60 50 40 30 20 10 0 10 20 30 40 50 60 70

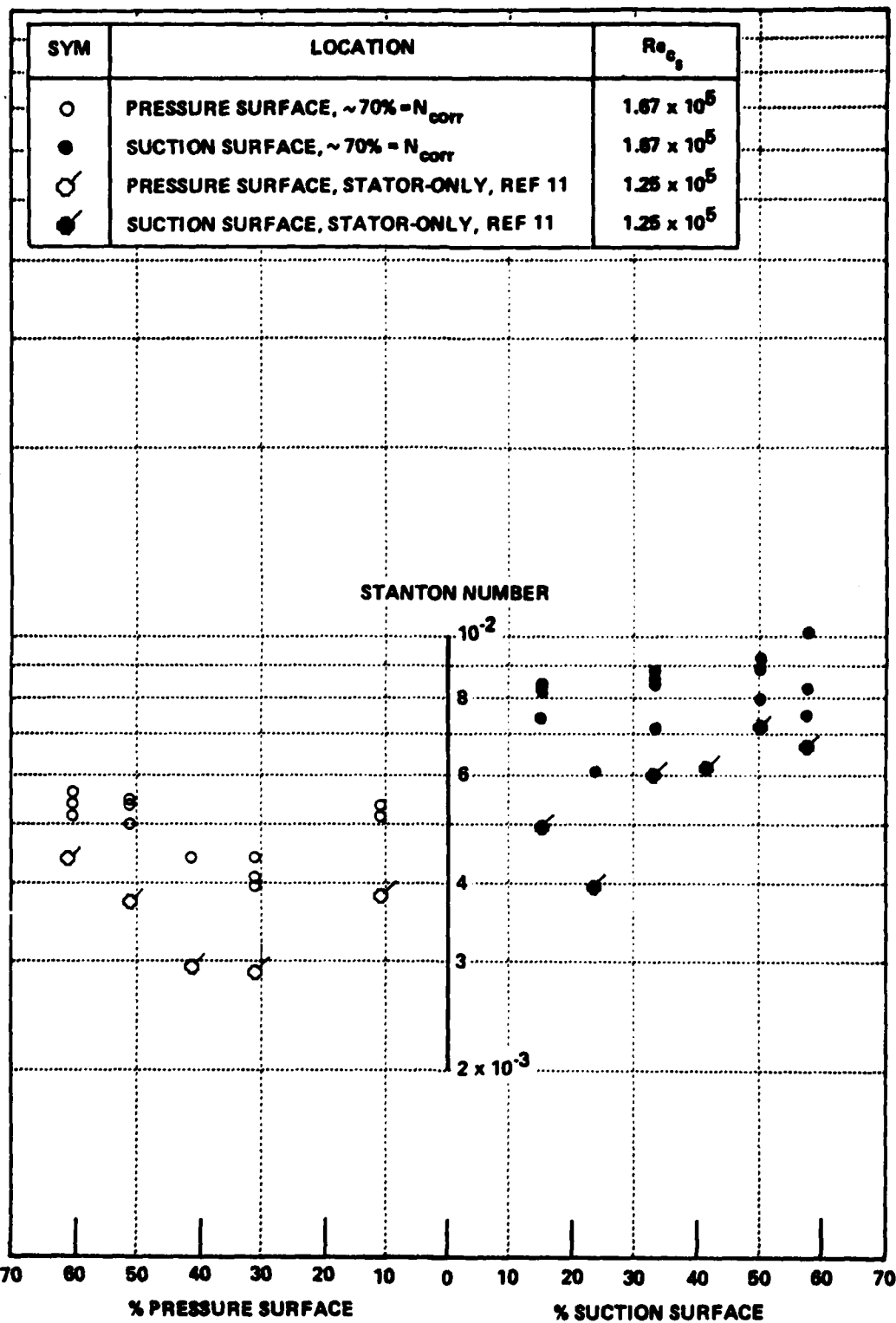% PRESSURE SURFACE   % SUCTION SURFACE

Figure 18 HEAT TRANSFER DISTRIBUTION ON STATOR AIRFOIL
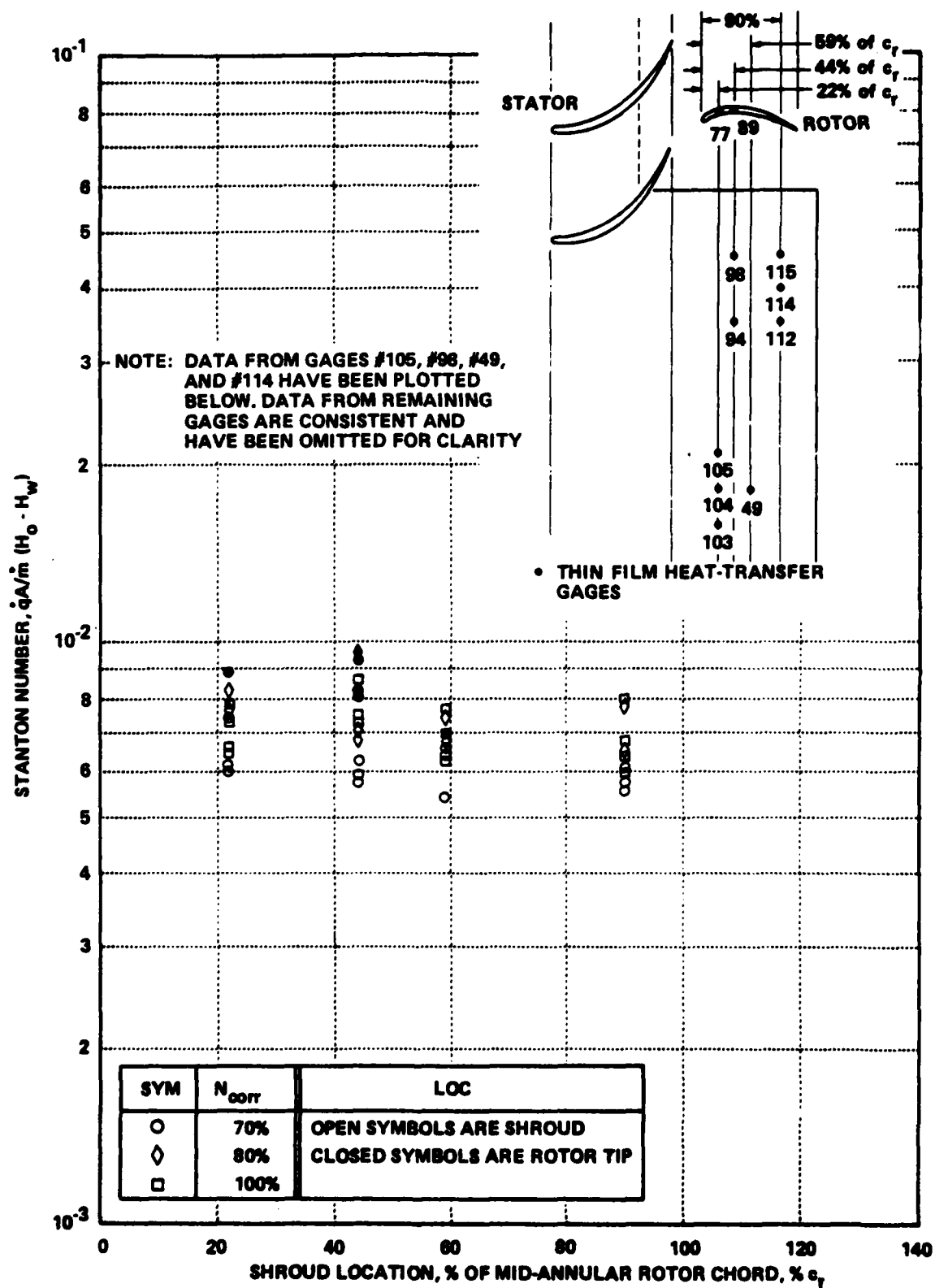
Figure 19   HEAT TRANSFER TO SHROUD AND ROTOR TIP

35

STATOR

ROTOR

85 86

98 115

114

94 112

$\dot{q}$

2 11

7 6 15 4 12

9 8

105

104 49

103

1 ms

TEST TIME

24,302 J/m²·sec
(248 BTU/ft²·sec)

N_{phy} = 21,740 rpm

N_{corr} = 78%

T_0 = 1011°K

Re_{cr} = 0.91 x 10⁵

$St \equiv \dot{q}A/\dot{m}(H_0 - H_w) = 6.55 \times 10^{-3}$

TIME

● CR-080 KULITE

• THIN FILM
  HEAT-TRANSFER GAGE
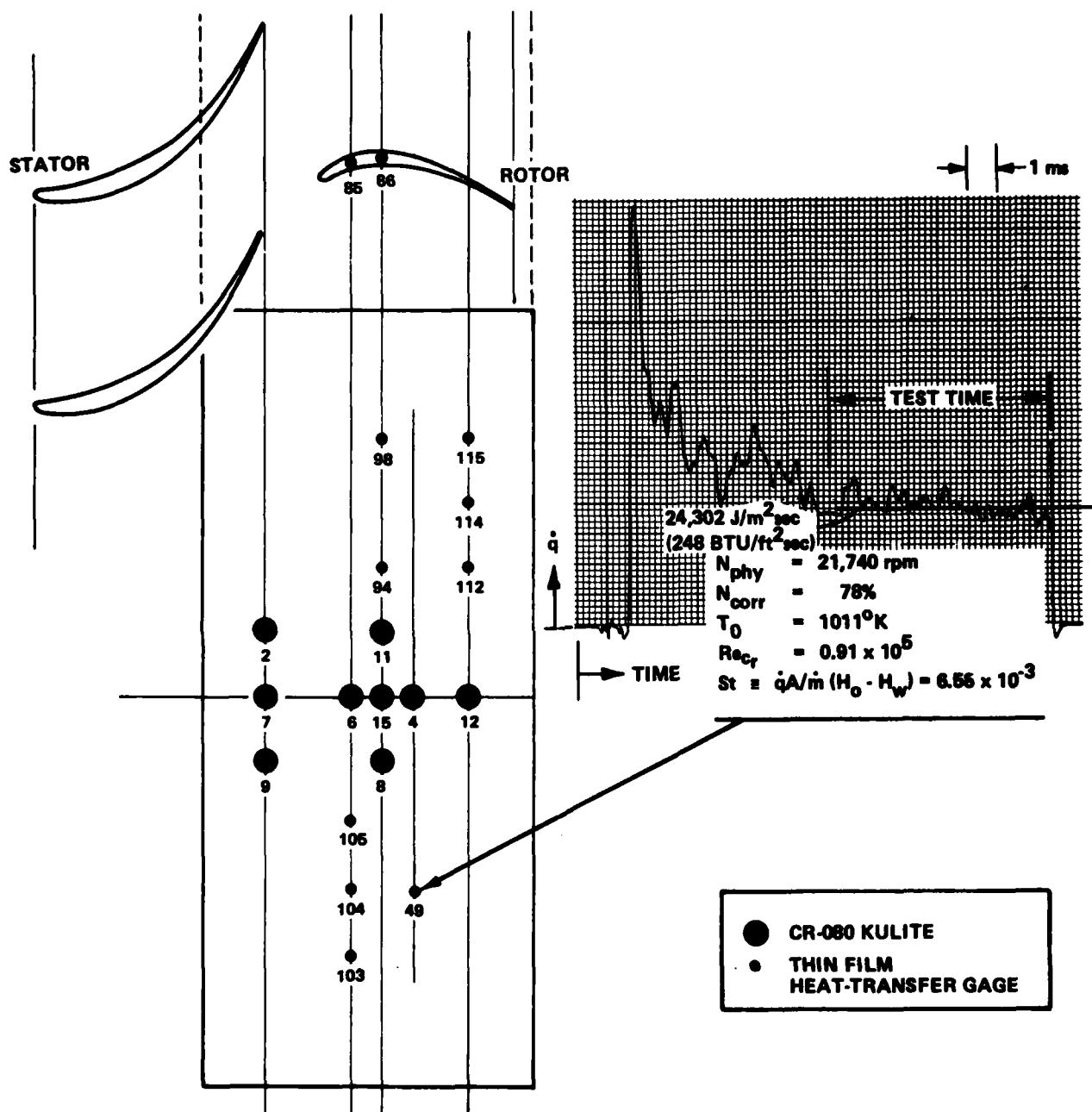
Figure 20   HEAT FLUX TO SHROUD

36

FLOW ESTABLISHMENT TIME

$\leftarrow$ 1 ms

TEST TIME

23,518 J/m²sec
(240 BTU/ft²sec)

N_{phy} = 21,740 rpm
N_{corr} = ~78%
T_0 = 1011°K
Re_{c_r} = 0.91 x 10⁵

$\dot{q}$

TIME

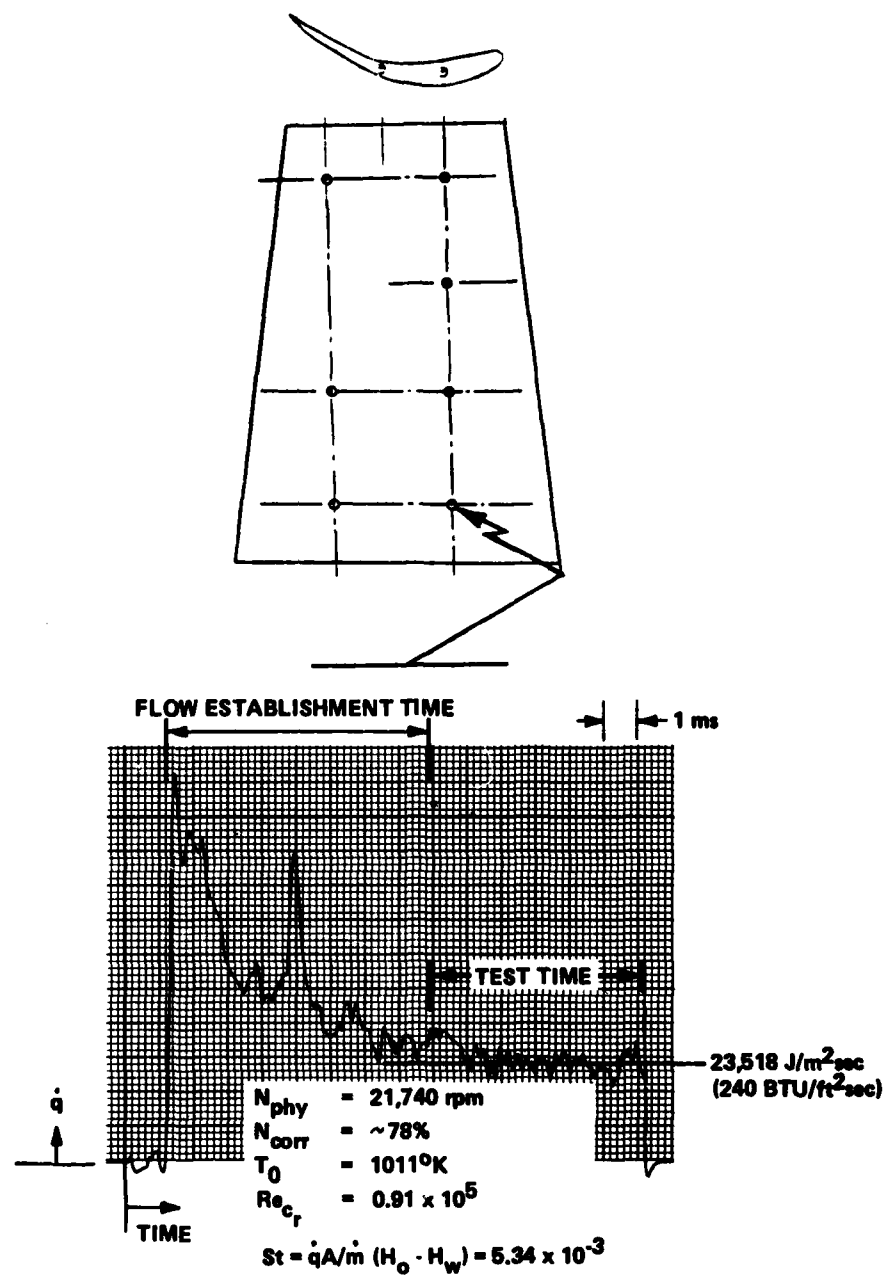$St = \dot{q}A/\dot{m}\,(H_o \cdot H_w) = 5.34 \times 10^{-3}$

Figure 21 HEAT FLUX TO ROTOR SUCTION SURFACE
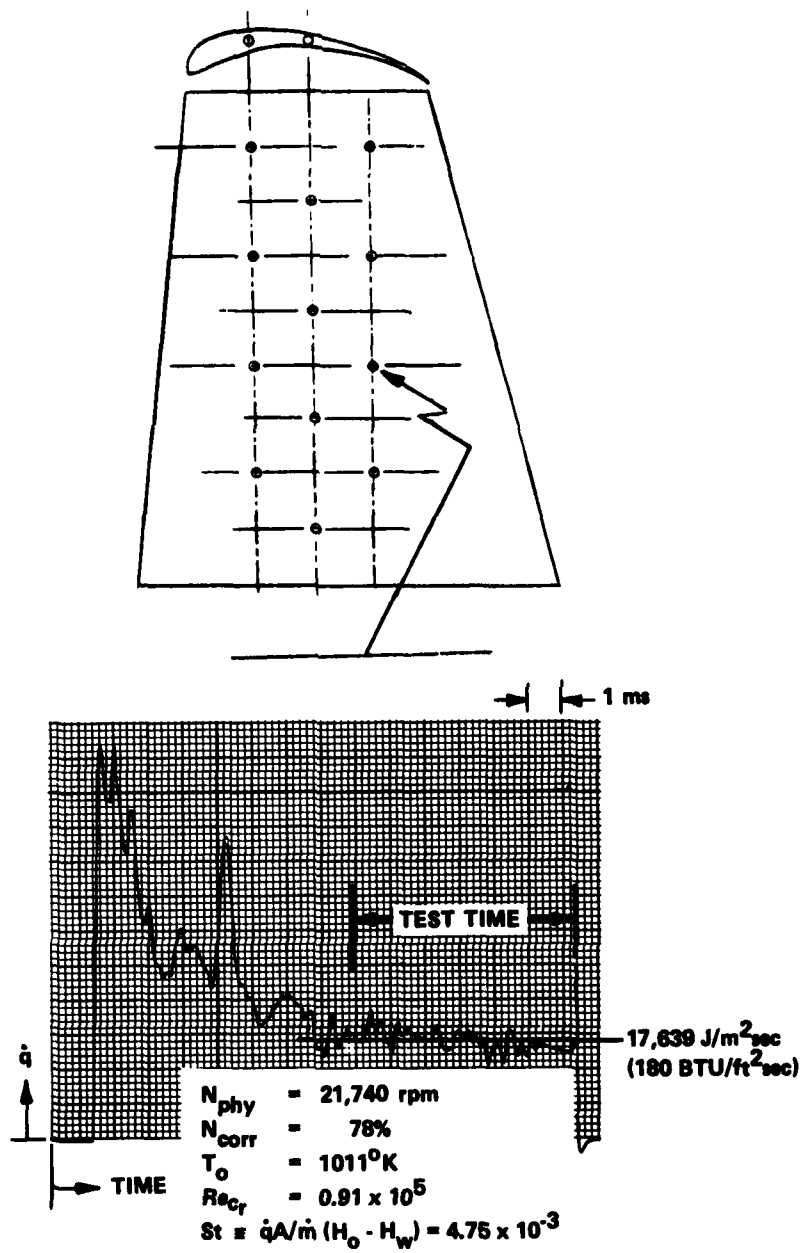
Figure 22   HEAT-FLUX TO ROTOR PRESSURE SURFACE

78 μsec

BASELINE

N_{phy} = 20,000 rpm
TIME FOR ROTOR PASSAGE THROUGH
STATOR WAKE = 73 μsec
BIOMATION SAMPLES EVERY 2.0 μsec
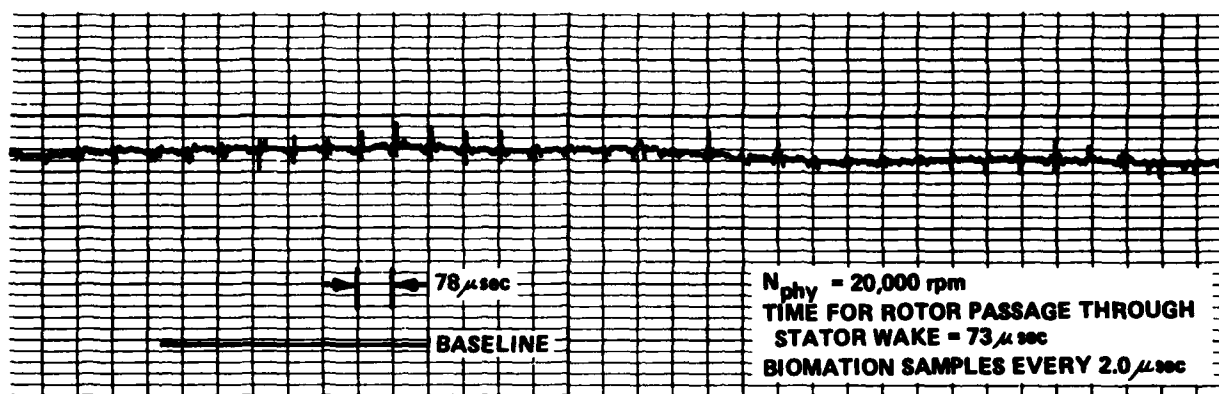
(a) GAGE #107 STATOR END WALL

78 μsec

BASELINE

N_{phy} = 20,000 rpm
TIME FOR ROTOR PASSAGE THROUGH
STATOR WAKE = 73 μsec
BIOMATION SAMPLES EVERY 2.0 μsec
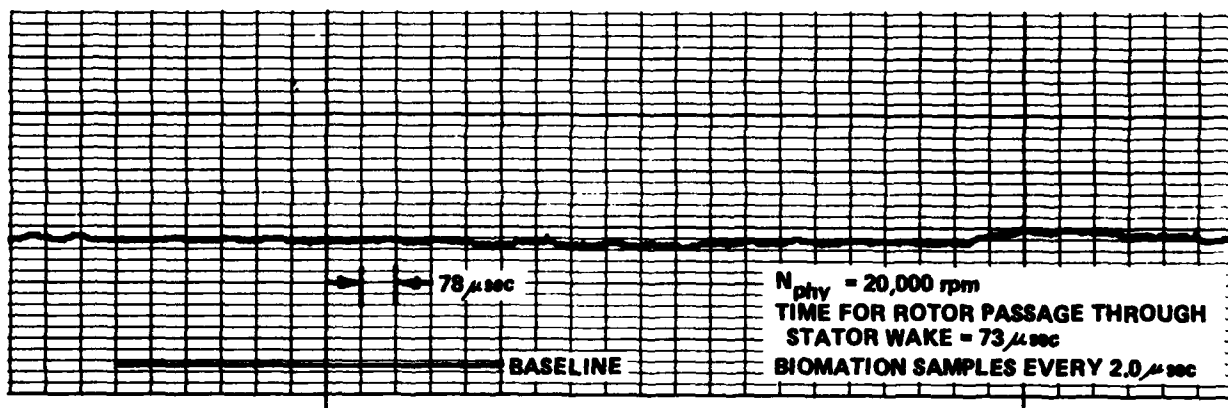
(b) GAGE #8-1 ROTOR SUCTION SURFACE

Figure 23   HEAT-FLUX GAGE TEMPERATURE HISTORY OBTAINED WITH
WAVEFORM RECORDER